CrossMark

Comparison of carbon cycle between the western Pacific subarctic and subtropical time-series stations: highlights of the K2S1 project

Makio C. Honda[1] · Masahide Wakita[1] · Kazuhiko Matsumoto[1] · Tetsuichi Fujiki[1] · Eko Siswanto[1] ·
Kosei Sasaoka[1] · Hajime Kawakami[1] · Yoshihisa Mino[2] · Chiho Sukigara[2] · Minoru Kitamura[1] · Yoshikazu Sasai[1] ·
Sherwood L. Smith[1] · Taketo Hashioka[1] · Chisato Yoshikawa[1] · Katsunori Kimoto[1] · Shuichi Watanabe[1] ·
Toru Kobari[3] · Toshi Nagata[4] · Koji Hamasaki[4] · Ryo Kaneko[4] · Mario Uchimiya[5] · Hideki Fukuda[4] · Osamu Abe[2] ·
Toshiro Saino

Abstract A comparative study of ecosystems and biogeochemistry at time-series stations in the subarctic gyre (K2) and subtropical region (S1) of the western North Pacific Ocean (K2S1 project) was conducted between 2010 and 2013 to collect essential data about the ecosystem and biological pump in each area and to provide a baseline of information for predicting changes in biologically mediated material cycles in the future. From seasonal chemical and biological observations, general oceanographic settings were verified and annual carbon budgets at both stations were determined. Annual mean of phytoplankton biomass and primary productivity at the oligotrophic station S1 were comparable to that at the eutrophic station K2. Based on chemical/physical observations and numerical simulations, the likely "missing nutrient source" was suggested to include regeneration, meso-scale eddy driven upwelling, meteorological events, and eolian inputs in addition to winter vertical mixing. Time-series observation of carbonate chemistry revealed that ocean acidification (OA) was ongoing at both stations, and that the rate of OA was faster at S1 than at K2 although OA at K2 is more critical for calcifying organisms.

1 Introduction

The "biological pump" is one of the important mechanisms by which atmospheric CO_2 is taken up by the ocean and transported to the ocean's interior, e.g., the concentration of atmospheric CO_2 would have risen to ~460 ppm from the pre-industrial value of ~280 ppm in the absence of the biological pump (Volk and Hoffert 1985). The biological pump transported ~13 gigatons of carbon (GTC) per year (year^{-1}) during the 2000s, during which time emissions of anthropogenic CO_2 were ~9 GTC year^{-1} (The Intergovernmental Panel on Climate Change [IPCC] 2013). However, recent increases of atmospheric CO_2 and associated global warming have caused warming, stratification, deoxygenation, and acidification of the ocean. There is now great concern that these changes of the ocean environment (multi-stressors) will affect the biological pump and its ability to mitigate increases of atmospheric CO_2 in the future. Computer simulations have predicted possible future changes in factors that influence the biological pump, such as the ratio of the export carbon flux to primary production (ef-ratio) (Laws et al. 2000), primary productivity (Bopp et al. 2001; Doney 2006), abundance and species of phytoplankton (Moran et al. 2010; Bopp

✉ Makio C. Honda
hondam@jamstec.go.jp

1 Japan Agency for Marine-Earth Science and Technology, 2-15 Natsushima-cho, Yokosuka 237-0061, Japan

2 Nagoya University, Furo, Chikusa, Nagoya 464-8601, Japan

3 Kagoshima University, 4-50-20, Shimoarata, Kagoshima 890-0056, Japan

4 The University of Tokyo, 5-1-5, Kashiwanoha, Kashiwa, Chiba 277-8564, Japan

5 RIKEN, 1-7-22 Suehiro, Tsurumi, Yokohama, Kanagawa 230-0045, Japan

et al. 2005), CaCO$_3$ production and particulate organic carbon (POC) vertical transport (Heinze 2004), depth of decomposition of POC (Kwon et al. 2009), production of dissolved organic carbon (DOC) and transparent exopolymers (TEP) (Arrigo 2007), and nitrate uptake (Smith 2011). Based on an inter-comparison of mathematical simulations (Coupled Model Intercomparison Project 5: OCMIP5) of future changes of ocean ecosystems caused by multiple stressors, Bopp et al. (2013) projected that global primary productivity in the late twenty-first century (2090–2099) would decrease by ~9 ± 8% from the rate in the late twentieth century (1990–1999) and that this change would be accompanied by a decrease of export production. However, as numerous authors have reported, changes of oceanic conditions will affect the biological pump and biogeochemistry differently in different locations in the ocean (Bopp et al. 2001, 2005, 2013; Gregg et al. 2003; Heinze 2004; Doney 2006; Kwon et al. 2009). Recently, Boyd et al. (2015) mathematically simulated future changes of multiple stressors, including iron (Fe) input. They also reported that the magnitude and effect of these multi-stressors on biogeochemistry would differ from one location to another. It is thus of great concern that an assessment be made of the current situation and a precise determination be made of any changes of the biological pump and biogeochemistry caused by changes of the ocean environment in the western North Pacific.

It is well known that the North Pacific Western Subarctic Gyre (WSG) is a terminal area of deep water circulation. The WSG is, therefore, rich in nutrients, the result being that the area is highly productive. Diatoms are the predominant algal taxon and have been reported to play an important role in the biological pump (e.g., Honda 2003; Buesseler et al. 2007, 2008). However, as described above, changes in the physics and chemistry of the ocean might change the ecosystem and biological pump in the western North Pacific. Previous studies have reported decreases of subsurface dissolved oxygen (Andreev and Watanabe 2002; Watanabe et al. 2008), net community productivity (Ono et al. 2002), primary productivity from 1950 to 2000 (Chiba et al. 2008), CaCO$_3$ flux from 1970 to 2000 (Watanabe et al. 2014), pH from 1997 to 2011 (Wakita et al. 2013), and an increase of small phytoplankton between 1970 and 2011 (Ishida et al. 2009). However, it is not known whether these changes are caused by global/ocean change or decadal variability such as Pacific Decadal Oscillation (PDO: Mantua et al. 1997). Hashioka et al. (2009) used a numerical simulation to investigate how primary productivity might change in a "high CO$_2$ world" in the western Pacific. They pointed out the possibility that the spring bloom would occur earlier and that phytoplankton biomass would increase in some areas. However, there has been little data to validate their prediction.

In the subarctic Pacific, interdisciplinary time-series geochemical observations have been conducted previously in the western Pacific (station KNOT; e.g., Saino et al. 2002) and eastern Pacific (station OSP; e.g., Harrison et al. 1999), and general oceanographic conditions were assessed. Although both chemical and biological (zooplankton and bacteria) observations were made at KNOT (e.g., Liu et al. 2002; Mochizuki et al. 2002; Yamaguchi et al. 2002), the role of related processes in the carbon cycle received little attention. In addition, because KNOT is located at the southwestern edge of the WSG (44°N, 155°E) and close to the Kuril Islands, KNOT is sometimes affected by subtropical water or coastal water and is not necessarily representative of oceanographic conditions in the WSG (e.g., Tsurushima et al. 2002; Harrison et al. 2004). Prior to our study, Buesseler et al. (2007, 2008) conducted a comparative study, the "VERTIGO project", at station K2 and subtropical station ALOHA (see below). That study revealed the mechanism of carbon transport to the ocean interior by taking into account both chemical and biological oceanography. However, observation at respective stations was conducted only in the summer in different years, and seasonal variability at both stations was not addressed. Between the early 1980s and middle 2000s, time-series observations at OSP, which is located in the Alaskan gyre of the eastern Pacific (50°N, 145°W), provided comprehensive information on oceanographic conditions in the subarctic Pacific (e.g., Harrison et al. 1999). In addition, the impact of ocean warming and future changes in Fe supply on the biogeochemistry of the region has been mathematically simulated (Denman and Pena 2002). However, the oceanography is very different at OSP and in the WSG with respect to nutrient supply (Wong et al. 2002a), phytoplankton ecology (Harrison et al. 2004), CO$_2$ exchange (Zeng et al. 2002), primary productivity (Harrison et al. 1999; Imai et al. 2002; Matsumoto et al. 2014), carbon export (Honda et al. 2002), and the magnitude and impact of Fe deficiency (Tsuda et al. 2003). In addition, decadal variability such as the PDO affects meteorology and physical oceanography in opposite ways in the western and eastern Pacific (e.g., Mantua et al. 1997).

Time-series observations in the subtropical Pacific have been conducted since the late 1980s as part of the United States's Hawaiian Ocean Time-series study (HOT) (e.g., Karl et al. 2001). At time-series station ALOHA (22°45′N, 158°W) off Hawaii, interdisciplinary oceanographic studies have been conducted on almost a monthly basis by using a research vessel and moored systems to carry out replicate field observations. However, this time-series study does not always reflect biogeochemistry in the middle of the subtropical Pacific (~30°N) because at ALOHA the winter mixed layer is very shallow (<125 m), nutrient (nitrate) concentrations are quite low (<0.01 μmol kg^{-1}), and atmospheric nitrogen fixation is one of the important sources of inorganic nitrogen in surface waters (Karl et al. 2001). In

addition, net primary productivity at ALOHA (~460 mg-C m^{-2} day^{-1}; Karl et al. 2001) has been determined by dawn-to-dusk incubations and must, therefore, be higher than that determined by 24-h incubations (Karl et al. 1996). Thus, although time-series observations have been conducted previously in the subarctic and subtropical areas in the North Pacific, there have been few biogeochemical time-series studies in the western Pacific based on nearly simultaneous comparative observations with the same methods.

To collect essential baseline data about this ecosystem and its biological pump to facilitate predictions of changes of material cycles via biological activity, a comparative study of the ecosystem and its biogeochemistry was planned at time-series stations set in the WSG (station K2) and subtropics (station S1). These two regions are characterized by different physical, chemical, and biological oceanography and are subjected to diverse allochthonous forcing, including seasonal monsoons, mesoscale eddies, and eolian inputs. This time-series study entitled "Study of Change in Ecosystem and Material Cycles Caused by Climate Change and its Feedback: K2S1 Project" was conducted with seasonal scientific cruises of the R/V *Mirai*, time-series observations made with a mooring system, satellite data analysis, and numerical simulations. This report provides a summary of the oceanographic settings, a compilation of the carbon budgets and scientific highlights at both stations. Details are provided mainly in papers in the *Journal of Oceanography* special issue "K2S1 project" [vol 72 (3), 2016].

2 Sampling and methods

2.1 Time-series stations

The subarctic time-series station K2 (47°N, 160°E; water depth 5300 m) was established in 2001 (Fig. 1a). Station K2 is located in the WSG and is characterized by a dicothermal layer (subsurface temperature minimum layer) that is formed in winter and persists in other seasons (Uda 1963); density is mainly determined by salinity (Fig. 1b). With some hiatuses, various observational studies have been conducted with research vessels and mooring systems, and the characteristics of settling particles, nutrients, phytoplankton and zooplankton have been reported previously (Honda et al. 2006,; Honda and Watanabe 2007; Honda et al. 2009; Honda and Watanabe 2010; Buesseler et al. 2007, 2008; Kawakami and Honda 2007; Kawakami et al. 2007; Wilson et al. 2008; Steinberg et al. 2008a, b; Kobari et al. 2008, 2013; Fujiki et al. 2014; Matsumoto et al. 2014; Kawakami et al. 2015).

As the counterpart of station K2, subtropical time-series station S1 (30°N, 145°E; water depth 5800 m) was established in 2010 (Fig. 1a). Sub-Tropical Mode Water (STMW) is formed in this area (e.g., Suga and Hanawa 1990). STMW, the temperature, salinity and sigma-theta of which are ~16 °C, 34.7 and 25.5, respectively, can be seen on the temperature-salinity (T-S) diagram for S1 (Fig. 1b). This station is also characterized by the
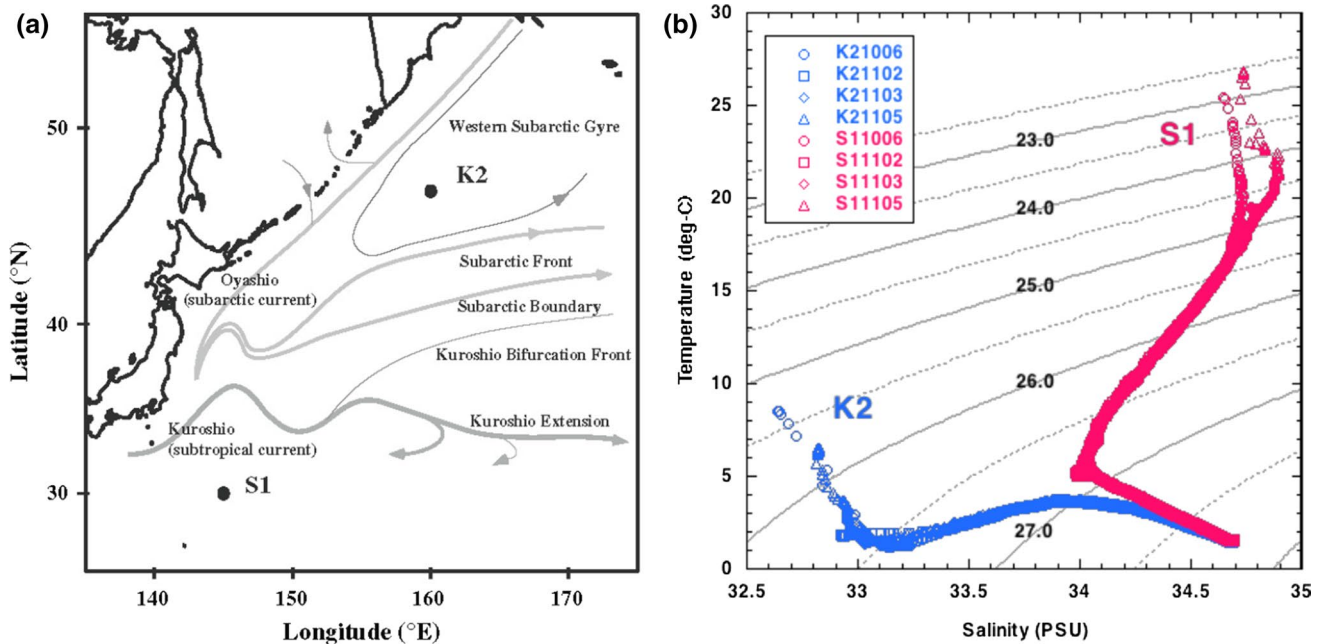

Fig. 1 **a** Time-series stations K2 and S1 (Kawakami et al. 2014), **b** T-S diagram at K2 and S1. Data were obtained by CTD observations during cruises MR10-06 (autumn), MR11-02 (winter), MR11-03 (spring), and MR11-05 (summer). Isopycnal lines (sigma-theta) are also shown

presence of North Pacific Intermediate Water (NPIW), which originates in the mesopelagic and is associated with a minimum salinity layer at a sigma-theta of ~26.8 (Reid 1965). In addition, the fact that temperature is the principal determinant of density (Fig. 1b) is one of the characteristics of this subtropical water. As described later, this area of the ocean is oligotrophic. However, Limsakul et al. (2002) have reported that primary productivity increases in the spring after vigorous winter mixing. Our observations indicated that S1 was just as productive as K2 (see below).

2.2 Scientific cruises and observations

Since January 2010, scientific cruises by the R/V *Mirai* have been conducted seven times (Table 1) as a part of the K2S1 project. During each cruise, the following measurements and analyses were carried out:

- Dissolved components (salinity, oxygen, nutrients, pH, total dissolved inorganic carbon: DIC, total alkalinity: TALK, pCO_2, dissolved organic carbon: DOC).
- Phytoplankton pigments by Turner fluorometer, high-performance liquid chromatography (HPLC), and chemotaxonomic analysis (CHEMTAX program).
- Primary productivity by in situ and simulated in situ incubations with ^{13}C, oxygen, and fast repetition rate fluorometry (FRRF).
- Zooplankton biomass and community structure by depth-stratified samplings using Intelligent Operated NEt Sampling System (IONESS) and North Pacific Standard net (NORPAC).
- Protozoan biomass by water sample collections using CTD-CMS.
- Viruses and heterotrophic nanoflagellates: abundance, and their role in microbial dynamics.
- Settling particles: seasonal and vertical variability in flux and chemical composition with drifting sediment traps in the upper 200 m, and bottom-tethered, time-series sediment traps below 200 m.
- Suspended particles, $POC_{(sus)}$, with in situ pumping system.
- Physical oceanography by conductivity-temperature-depth measurements.

In addition, during the MR11-05 cruise (July 2011), to elucidate the relationship between meso-scale eddies and ocean primary productivity/the biological pump, multiple drifting profiling floats (ARGO floats), each with a dissolved oxygen sensor, were deployed near station S1. The results of this intensive study, named "S1-INBOX", have been reported elsewhere (Inoue et al. 2016a, b; Kouketsu et al. 2016a, b). Besides oceanographic observations,

satellite data analysis and numerical simulations were conducted to elucidate inter-annual and decadal variability in meteorology and oceanography, to clarify the mechanisms associated with the cycling of materials at these stations.

2.3 Estimation of carbon budget

In this study, carbon budgets in the annual maximum surface mixed layer (SML) and mesopelagic layer (MPL: from bottom of the SML to 1000 m) at both stations were determined using previously reported results and new data such as DIC, TALK, DOC, phytoplankton biomass and primary productivity, zooplankton/prokaryote biomass and carbon demand and settling particles. Most of the data are available on the "K2S1 database" (http://ebcrpa.jamstec.go.jp/k2s1/en/). Detail procedures used to estimate the principal components of the carbon budgets are described in Online Appendix 1.

3 Oceanographic settings of K2 and S1

Figure 2a–r shows the seasonal variability of important parameters at K2 and S1. To understand seasonal variability at a decadal timescale, we used hydrographic observation data (Fig. 2a–h, k, l) at K2 and S1 obtained during other cruises from 2004 to 2013 (Japan Agency for Marine-Earth Science and Technology [JAMSTEC], Japan Meteorological Agency [JMA], and WOCE-P2) in addition to K2S1 project data. Moreover, data obtained by other cruises, ARGO profiling float data (ARGO float mixed layer grid point values [MILA GPV] during 2001–2010; Hosoda et al. 2010), climatological data (World Ocean Atlas 2009 [http://www.nodc.noaa.gov/OC5/WOA09/pr_woa09.html]; hereinafter WOA 2009), and satellite data are also shown in some figures to elucidate the seasonal variability of some parameters. We sorted the data by month without regard to observation year because inter-annual variability of oceanographic conditions in these areas is much smaller than seasonal variability (Wakita et al. 2013). Details of seasonal variability in respective components are documented in Online Appendix 2. Major characteristics of oceanographic settings at both stations are shown in Table 2 and can be summarized as follows:

(a) Mixed layer depth (MLD) at S1 was larger than that at K2 (Fig. 2a, b).
(b) Water temperature at S1 was always about 15 °C higher than that at K2 (Fig. 2b, c).
(c) Salinity at S1 was about 1.5 times higher than that at K2 (Fig. 2e, f).
(d) K2 (S1) was the source (sink) of CO_2 in winter and the sink (source) of CO_2 in summer (Fig. 2g, h).

Table 1 Scientific cruises for the K2S1 project and principal onboard observations

Cruise name		Cruise period (UTC)	Date of Stay (UTC) K2 (47N/160E)	Date of Stay (UTC) S1 (30N/145E)	Routine K2	Routine S1	Pigment K2	Pigment S1	Primary productivity K2	Primary productivity S1	Zooplankton (IONESS) K2	Zooplankton (IONESS) S1	Prokaryote abundance and heterotrophic production K2	Prokaryote abundance and heterotrophic production S1	Drifting sediment trap K2	Drifting sediment trap S1	ST mooring K2	ST mooring S1	POPPS mooring K2	POPPS mooring S1
MR10-01	Leg.1	19 Jan 2010–6 Feb 2010	23 Jan 2010–26 Jan 2010	30 Jan 2010–4 Feb 2010	O	O	O	O	O	O	O	O	O	O	O	O	R	D	D	D
	Leg.2	7 Feb 2010–24 Feb. 2010	13 Feb 2010–16 Feb 2010	8 Feb 2010–10 Feb 2010	O	O	O	O	O	O	O	O	-	-	-	O	D	-	-	-
MR10-06		18 Oct 2010–16 Nov 2010	24 Oct 2010–1 Nov 2010	6 Nov 2010–12 Nov 2010	O	O	O	O	O	O	O	O	O	O	O	O	R,D	R,D	R*	R,D
MR11-02		11 Feb 2011–9 Mar 2011	25 Feb 2011–2 Mar 2011	13 Feb 2011–19 Feb 2011	O	O	O	O	O	O	O	O	-	-	O	O	-	-	-	-
MR11-03		14 Apr 2011–5 May 2011	19 Apr 2011–23 Apr 2011	28 Apr 2011–3 May 2011	O	O	O	O	O	O	O	O	O	O	O	O	-	-	-	-
MR11-05	Leg.1	26 Jun 2011–17 Jul 2011	29 Jun 2011–8 Jul 2011	-	O	-	O	-	O	-	O	-	O	-	O	-	R,D	-	-	-
	Leg.2	17 Jul 2011–4 Aug 2011	-	23 Jul 2011–31 Jul 2011	-	O	-	O	-	O	-	O	-	O	-	O	-	R,D	-	R,D
MR12-02	Leg.1	4 Jun 2012–24 Jun 2012	9 Jun 2012–15 Jun 2012	-	O	-	O	-	O	-	O	-	O	-	O	-	R,D	-	-	-
	Leg.2	24 Jun 2012–12 Jul 2012	-	25 Jun 2012–2 Jul 2012	-	O	-	O	-	O	-	O	-	O	-	O	-	R,D	-	R,D
MR13-04		9 Jul 2013–28 Jul 2013	21 Jul 2013–24 Jul 2013	13 Jul 2013–17 Jul 2013	O	O	O	O	O	O	O	O	-	-	-	-	R,D	R,D	-	R,D

Underlined cruises were "core" seasonal cruises, and data obtained during these cruises were used for estimating annual averages in Fig. 3 and Table 3

R and D for moorings denote Recovery and Deployment, respectively

* K2-POPPS mooring were recovered by other ship in May 2010

(e) Annual mean of photosynthetic active radiation (PAR) at S1 was about 1.5 times higher than that at K2 (Fig. 2i, j).

(f) Nutrient (nitrate and nitrite: NOx) at S1 was less than 1.5 µmol kg^{-1} even in winter and very low or below detection limit during other seasons (Fig. 2k, l).

(g) Although nutrient was very low at S1, difference in annual mean of integrated chlorophyll-*a* (IChl-*a*) between two stations was small (Fig. 2m, n).

(h) Diatom was pre-dominant of phytoplankton during many seasons at K2 while smaller phytoplankton such as *Prochlorococcus* was pre-dominant during many seasons at S1 (Fig. 2o, p).

(i) Annual mean of integrated primary productivity (IPP) at S1 was comparable to or slightly higher than that at K2 despite of lower nutrient at S1 (Fig. 2q, r).

4 Highlights of K2S1 project

4.1 Carbon budget

Figure 3a, b and Table 2 show the annual average of the carbon balance in the SML and in the MPL at K2 (Fig. 3a) and S1 (Fig. 3b). Note that observations indicate that the SML extends from the surface to 150 m at K2 and to 200 m at S1. Averages of variables were estimated mainly with data obtained from cruises MR10-06, MR11-02, MR11-03, and MR11-05 (Table 1). Although the inputs and outputs of carbon from the various boxes in Fig. 3 are not necessarily balanced, this depiction of the carbon balance was constructed from the perspective of marine chemistry and biology. In the future, this figure will hopefully be used to validate numerical models and simulate future changes. It is, however, noted that some numbers are not always same as numbers in original papers due to the difference in target period and depth: for example, IPPs at K2 (S1) were estimated to be 315 (369) mg-C m^{-2} day^{-1} based on data obtained from R/V *Mirai* core cruises (Table 3) (this study), whereas the IPPs at K2 (S1) were estimated to be 292 (303) mg-C m^{-2} day^{-1} (Table 2) based on data from every cruise in Table 1 (Matsumoto et al. 2016). Principal points relative to the carbon balance are as follows:

4.1.1 Dissolved inorganic and organic carbon

The annual mean CO_2 net influx (CO_2 flux from the atmosphere to the ocean) at K2 was estimated to be 27.3 ± 8.2 mg-C m^{-2} day^{-1} (Table 3). This influx is comparable to the influx of ~23 mg-C m^{-2} day^{-1} at OSP (Wong and Chan 1991). At S1, the annual mean CO_2 net influx was estimated to be 46.7 ± 14.1 mg-C m^{-2} day^{-1}. This

influx was ~1.6 times that at K2 and about twice the influx of ~23 mg-C m^{-2} day^{-1} at ALOHA (Winn et al. 1994). This difference might be caused by to the production of STMW near S1 and the transport of more surface water CO_2 to the ocean interior (IPCC 2013). Detail is reported in Wakita et al. (2016).

Entrainment of DIC from the MPL by diffusion at K2 and S1 was estimated to be 28.3 and 47.7 mg-C m^{-2} day^{-1}, respectively (Fig. 3a, b; Table 3). This vertical diffusive flux at S1 was ~1.5 times that at K2, mainly due to the larger vertical diffusivity at S1 (K2: 3.5×10^{-5} m^2 s^{-1}, S1: 2.0×10^{-4} m^2 s^{-1}, Wakita et al. 2016). The sum of DOC output estimated by diffusion, prokaryote carbon demand (Prok CD), and mineralization (i.e., conversion to DIC: this is the annual DOC flux of -0.68 mol-C m^{-2} year^{-1} reported by Wakita et al. 2016) at K2 was estimated to be 170 mg-C m^{-2} day^{-1} (1 + 147 + 22, respectively; Fig. 3a). The analogous sum of DOC output at S1 was estimated to be 195 mg-C m^{-2} day^{-1} at S1 (8 + 166 + 21, respectively; Fig. 3b), comparable to or slightly higher than that at K2. It is noteworthy that a little DOC at both stations was exported to the MPL.

4.1.2 Phytoplankton biomass and primary productivity

The estimated phytoplankton biomass of 3006 ± 595 mg-C m^{-2} at K2 was comparable to that at S1, 3229 ± 1413 mg-C m^{-2} (Fig. 3a, b; Table 3).

The annual average of net primary productivity (NPP = IPP) at K2 was estimated to be 315 ± 39 mg-C m^{-2} day^{-1}, ~20% lower than that at S1 (369 ± 47 mg-C m^{-2} day^{-1}). Gross primary productivity (GPP) at S1 was estimated to be 825 ± 101 mg-C m^{-2} day^{-1}, 1.5 times that at K2 (536 ± 106 mg-C m^{-2} day^{-1}). As a result, the ratio of NPP to GPP at K2 (~0.59) was ~30% higher than the ratio at S1 (~0.44). We suspect that the sum of DOC production and respiration accounts for the differences between GPP and NPP. Based on the empirical relationship between DOC production and NPP (see Online Appendix 1), we estimated DOC production at K2 (S1) to be 17 ± 2 (79 ± 10) mg-C m^{-2} day^{-1} (Fig. 3; Table 3). Details of NPP and GPP and higher DOC production at S1 than K2 have been reported elsewhere (Matsumoto et al. 2016).

4.1.3 Settling particles

Observed POC fluxes at the bottom of the SML (150 m for K2 and 200 m for S1) were 48.0 ± 4.8 mg-C m^{-2} day^{-1} at K2 and slightly higher than that at S1 (36.4 ± 3.6 mg-C m^{-2} day^{-1}). This is supported by another observation that POC flux at 400 m estimated from ^{210}Po at K2 was higher than that at S1 (Kawakami et al. 2015). The observed Particulate Inorganic Carbon (PIC) flux at K2 was
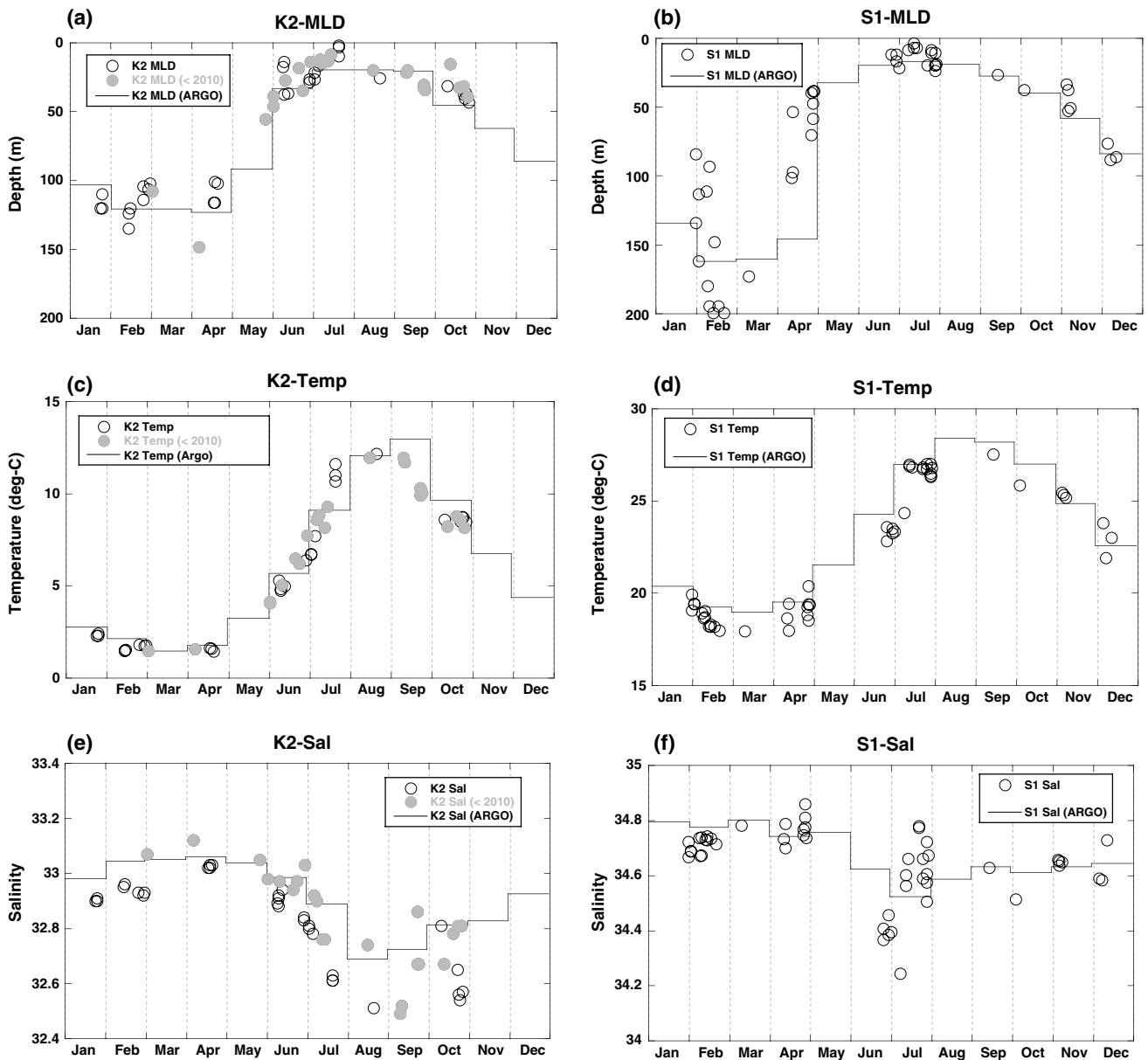
Fig. 2 Seasonal variability in **a b** MLD, **c d** water temperature, **e f** salinity, **g h** pCO$_2$ (partial pressure of CO$_2$) in the ML, **i j** surface PAR, **k l** average NO$_3$ + NO$_2$ in the ML, **m n** integrated chlorophyll-*a* (IChl-*a*) in the upper 200 m, **o p** phytoplankton composition in the euphotic layer: 1-dinoflagellates, 2–diatoms, 3-chlorophytes, 4-prymnesiophytes, 5-cryptophytes, 6-chrysophytes, 7-prasinophytes, 8-cyanobacteria, 9-prochlorophytes, and **q r** integrated primary productivity (IPP) in the ML for K2 and for S1, respectively. *Open circles* for both stations and *gray circles* for K2 are data observed during the K2S1 project (Table 1) and before this project, respectively. *Line graphs* in panels (**a**) through (**f**) are monthly averages of respective components around K2 and S1 obtained from mixed layer data of ARGO floats in MILA GPV, e.g., Hosoda et al. (2010). Line graphs in (**g**) and (**h**) are monthly averages of pCO$_2$ in air (pCO$_{2(air)}$) around K2 and S1 (zonal average of 48.6°N and 30°N, respectively, obtained

from NOAA Greenhouse Gas Reference: Dlugokency et al. 2014). Line graphs in panels (**i**) and (**j**) are climatological daily PAR around K2 and S1 obtained from MODIS data. Line graphs in panels (**k**) and (**l**) are monthly averages of NO$_3$ around K2 and S1 obtained from the WOA 2009. Data with *error bars* in panels (**m**) and (**n**) are climatological surface Chl-*a* concentrations obtained from the MODIS satellite between 2002 and 2012. Data with *error bars* in panels (**q**) and (**r**) are climatological IPP obtained from the MODIS satellite between 2002 and 2012 and using the VGPM model (Behrenfeld and Falkowski 1997). *Horizontal lines* in panels (**m**) and (**n**) for IChl-*a* and (**q**) and (**r**) for IPP are seasonal averages estimated with data from the four R/V *Mirai* "core" cruises (*thick lines*) and data from all cruises (*thin lines*) (Table 1). Note that scales of the *vertical axes* for temperature (**a**, **b**), salinity (**c**, **d**) and NO$_3$ + NO$_2$ (**k**, **l**) are different between stations
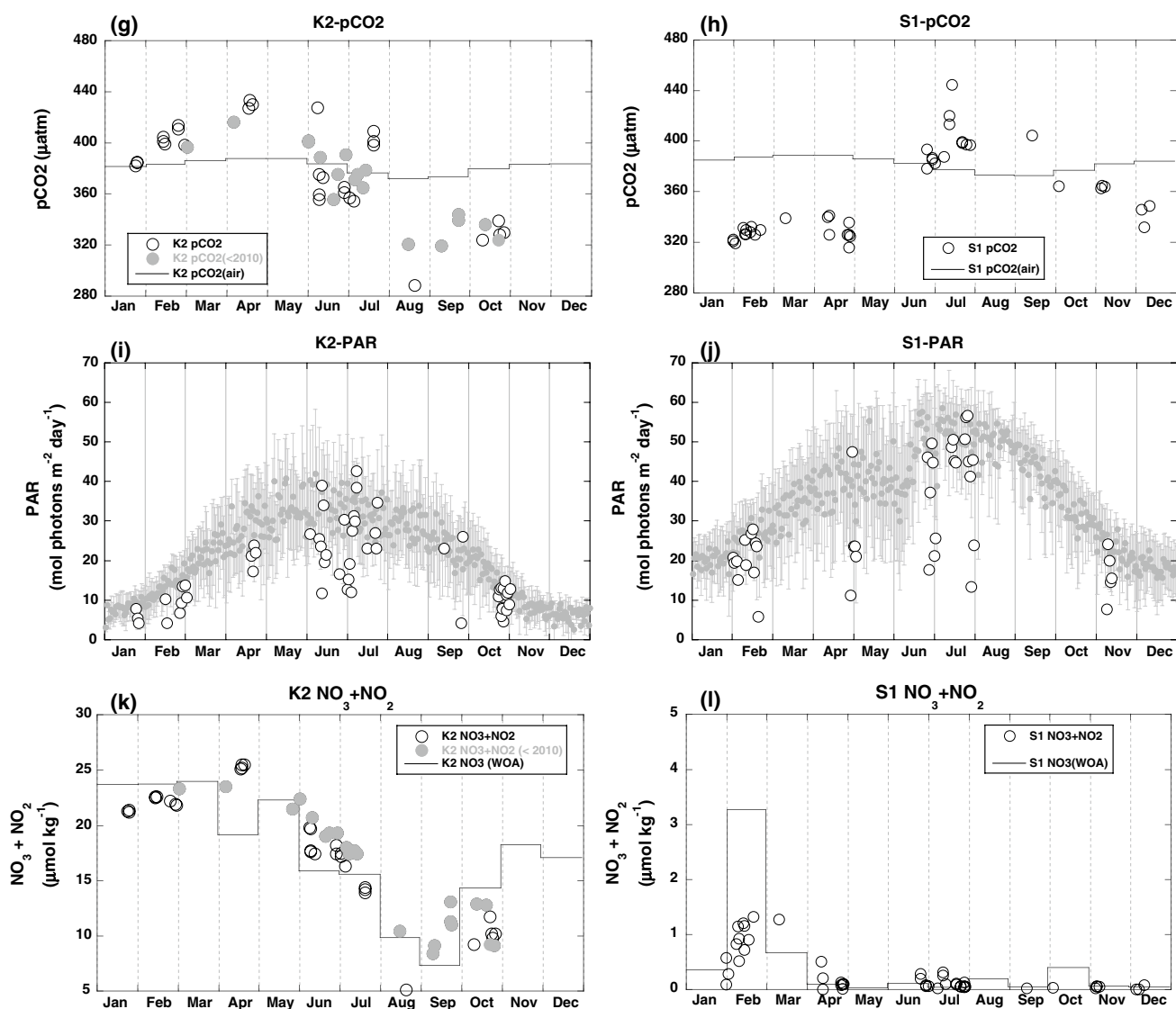
Fig. 2 continued

9.0 ± 0.9 mg-C m^{-2} day^{-1} and slightly lower than that at S1 (13.9 ± 1.4 mg-C m^{-2} day^{-1}). Based on the carbon balance, POC, and PIC fluxes were estimated to be 47 (82) and 7.2 (2.3) mg-C m^{-2} day^{-1}, respectively, at K2 (S1) (Wakita et al. 2016). These estimates are comparable to the fluxes observed with drifting sediment traps at K2, but inconsistent with those at S1 (Figs. 3a, b; Table 3). Fecal pellets comprised 1–40% of the POC flux at K2 and less than 3% at S1 (Kobari et al. 2016). Based on drifting sediment trap experiments, Wong et al. (2002b) reported that POC (PIC) fluxes at 200 m at OSP are ~53 (19) mg-C m^{-2} day^{-1}, the indication being that the POC flux at OSP is comparable to that at K2 and the PIC flux at OSP is higher than that at K2. At ALOHA, POC (PIC) fluxes at 150 m have been estimated to be 27.8 ± 10.3 (3.0 ± 1.7) mg-C m^{-2} day^{-1} based on archived data (HOT project database:

http://hahana.soest.hawaii.edu/hot/hot-dogs/pfextraction.html). Thus POC (PIC) fluxes at Station ALOHA are comparable to (lower than) those at S1.

POC and PIC fluxes at 4810 m at K2 were 5.7 ± 0.6 and 4.8 ± 0.5 mg-C m^{-2} day^{-1}, respectively, about twice those at S1 (POC: 2.0 ± 0.2 mg-C m^{-2} day^{-1}; PIC: 2.8 ± 0.3 mg-C m^{-2} day^{-1}). Assuming that POC and PIC fluxes decrease exponentially with depth (see Sect. 2.3.5), the interpolated POC (PIC) fluxes at 1000 m were estimated to be 15.0 ± 2.3 (6.4 ± 1.0) mg-C m^{-2} day^{-1} at K2, higher than those at S1 (POC: 9.3 ± 1.4 mg-C m^{-2} day^{-1}; PIC: 6.2 ± 0.9 mg-C m^{-2} day^{-1}) (Table 3). There is reason to suspect that the magnitudes of the rate of change with depth of the POC and PIC fluxes were larger at S1 than at K2 (Honda et al. 2016, K2S1 database). POC (PIC) flux at 1000 m and 3800 m at OSP were reported to 5.7 ± 3.4
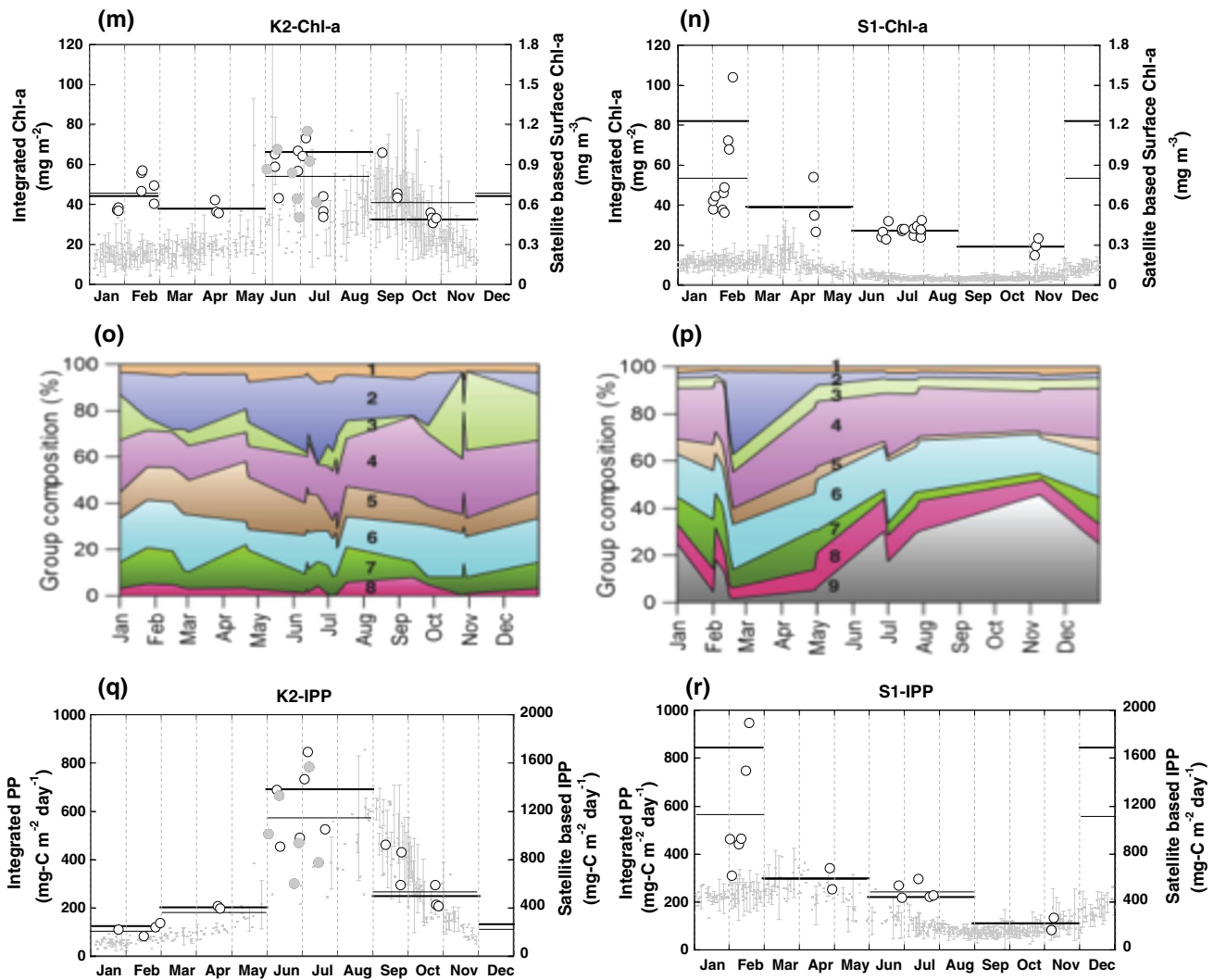
Fig. 2 continued

(5.3 ± 3.4) and 2.7 ± 1.9 (4.1 ± 2.4) mg-C m^{-2} day^{-1}, respectively (Timothy et al. 2013). Thus, POC flux at K2 was significantly higher than that at OSP and PIC flux was comparable to that at OSP.

4.1.4 Zooplankton biomass and carbon demand

At K2, biomass of mesozooplankton (or metazoans) in the SML and MPL were estimated to be 2734 ± 1370 and 2247 ± 159 mg-C m^{-2}, respectively. These are about one order of magnitude higher than those at S1 (276 ± 68 for SML and 298 ± 83 mg-C m^{-2} for MPL) (Table 3). This observation is noteworthy because phytoplankton biomass and primary productivity at shallow depths are comparable at K2 and S1, as noted before. Possible explanations are that (1) the respiratory and excretory carbon losses by large zooplankton at K2 are lower than

those by small zooplankton at S1 (2) the lower temperature at K2 leads to lower carbon loss by mesozooplankton, (3) the higher turnover rates of small zooplankton population at S1 keep biomass lower, and (4) dormant and non-feeding copepods, including *Eucalanus* and *Neocalanus*, which have longer life spans and accumulate lipids in their bodies, are dominant in the MPL at K2 (Kitamura et al. 2016).

Proto and metazoan carbon demand in the SML was estimated to total 279 (87 + 192) ± 122 mg-C m^{-2} day^{-1} at K2. It is noteworthy that proto- and metazoan carbon demand at S1 was estimated to be 257 (136 + 121) ± 55 mg-C m^{-2} day^{-1}, comparable to that at K2, although zooplankton biomass was much smaller at S1 than at K2. The carbon export flux from the SML to the MPL by mesozooplankton is the sum of ontogenetic migration, fecal pellet sinking, and active carbon

Table 2 Summary of Oceanographic settings at stations K2 and S1

			K2	S1	Note
Surface mixed layer depth (m)	Fig. 2a, b	annual maximum	⁓150	⁓200	OSP: < 125 ALOHA: < 125
Temperature (°C)	Fig. 2c, d	annual amplitude	⁓1.5–12	⁓18–28	
Salinity	Fig. 2e, f	annual amplitude	⁓32.5–33.3	⁓34.2–34.9	
$pCO_{2(sea)}$ (μatm)	Fig. 2g, h	annual amplitude	⁓300–440	⁓320–440	$pCO_{2(air)}$: ⁓390
			(Winter > Summer)	(Summer > Winter)	
Photosynthetically Active Radiation (mol photons m^{-2} day^{-1})	Fig. 2I, j	annual average	⁓17.5	⁓29.7	
Nitrate + Nitrite (μmol kg^{-1})	Fig. 2k, l	annual amplitude	⁓5–25	⁓0–2	OSP: ⁓5–15 ALOHA: < 0.01
Integrated Chlorophyll-a (mg m^{-2})	Fig. 2m, n	annual amplitude	⁓35–75	⁓20–105	
		annual average	⁓45	⁓34	OSP: ⁓23 ALOHA: ⁓23
Phytoplankton composition	Fig. 2o, p	Major species	diatom (late winter - early summer)	*Prochlococcus* (spring - autumn)	
			Prymnesiophytes (late summer - winter)	*Prymnesiophytes*, diatom (winter)	
Integrated Primary productivity (mg-C m^{-2} day^{-1})	Fig. 2q, r	annual amplitude	⁓100–850	⁓100–950	
		annual average	⁓292	⁓303	OSP: ⁓380–590 ALOHA: ⁓460 *

For comparison, some oceanographic settings at other time-series stations in the subarctic Pacific Ocean, stations OSP (Harrison et al. 1999), and the subtropical Pacific Ocean, station ALOHA (Letelier et al. 1996; Karl et al. 2001), are also shown. Details are described in Online Appendix 2

* Daytime incubation

flux (respiration and excretion in the MPL by diel vertical migratory zooplankton). At K2 that flux was estimated to be ~13.2 (2.3 + 7.0 + 3.9, respectively) mg-C m^{-2} day^{-1}, about two times the flux at S1 (5.2 = ~0 + 0.6 + 4.6, respectively) assuming that ontogenetic migration at S1 is quite smaller than that at K2. Export carbon flux by mesozooplankton was comparable to ~32 and 15% of the POC flux without fecal pellets at K2 and S1, respectively.

Mesozooplankton carbon demand in the MPL at K2 was estimated to be ~100 ± 4 mg-C m^{-2} day^{-1}. However, the carbon flux from the SML (sum of POC flux losses in the MPL: < 33.0 and zooplankton ontogenetic migration: 2.3 mg-C m^{-2} day^{-1}) did not satisfy mesozooplankton carbon demand. Mesozooplankton carbon demand at S1 was estimated to be 40 ± 11 mg-C m^{-2} day^{-1}. This carbon demand cannot be supported by the carbon flux from the SML either (sum of POC flux loss in the MPL: <27.1 and zooplankton ontogenetic migration: ~0 mg-C m^{-2} day^{-1} suspected above). Steinberg et al. (2008b) have also reported a mismatch between the carbon demand of

zooplankton and the POC flux based on observations during the summer at K2. In our study, this mismatch could not be explained at both K2 and S1, even when based on seasonal observations.

4.1.5 Prokaryote biomass and carbon demand

Unlike zooplankton, the difference in prokaryote (bacteria and archaea) biomass between the two stations was not large: 1280 ± 64 mg-C m^{-2} in the SML and 1440 ± 72 mg-C m^{-2} in the MPL at K2; 1030 ± 52 mg-C m^{-2} in the SML and 940 ± 47 mg-C m^{-2} in the MPL at S1 (Fig. 3a, b). Prokaryote carbon demand (DOC demand) in the SML was estimated to be 147 ± 19 mg-C m^{-2} day^{-1} at K2 and 166 ± 22 mg-C m^{-2} day^{-1} at S1. These demands can be supported sufficiently by the sum of DOC production in the SML (originating from phyto/zooplankton and prokaryotes). Prokaryote carbon demand in the MPL was estimated to be 13.9 ± 1.8 mg-C m^{-2} day^{-1} at K2 and 9.6 ± 1.2 mg-C

m^{-2} day^{-1} at S1. These values accounted for 27–41% of organic carbon delivery available for prokaryote consumption (attenuation of sinking POC flux + DOC diffusive export: <33.0 + 0.95 mg-C m^{-2} day^{-1} at K2 and <27 + 8.23 mg-C m^{-2} day^{-1} at S1) in the MPL. In addition, the flux of suspended matter or slowly sinking POC might be another potential source of DOC available for prokaryotes (Giering et al. 2014).

4.2 Missing source of nutrients at S1

As described before, the biomass of phytoplankton and primary productivity at S1 were unexpectedly high and comparable to those at K2, although the nutrient concentrations at S1 were very low. Based on comprehensive observation, it has been verified that the factors limiting primary productivity at S1 were the concentrations of major nutrients such as NO_3 (Matsumoto et al. 2016; Siswanto et al. 2015), whereas light (Matsumoto et al. 2014; Siswanto et al. 2015) and the micro-nutrient Fe (Fujiki et al. 2014) were limiting at K2.

Sasai et al. (2016) simulated the seasonal variability of primary productivity using a one-dimensional, physical-biological model. They successfully reproduced primary productivity during the winter productive season, when the SML was well developed, and nutrients were supplied to the euphotic zone. However, they underestimated primary productivity during the other seasons, when the ocean was strongly stratified and the supply of nutrients was inadequate. They also pointed out that the annual uptake ratio of NO_3 to $NO_3 + NH_4$ (f-ratio) at S1 was ~0.3, lower than the ratio at K2 (~0.5). It is, therefore, possible that phytoplankton at S1 uses more regenerated NH_4 instead of NO_3 than at K2. It has been reported that regenerated production accounts for most primary production at ALOHA (Karl et al. 1997).

Regenerated NH_4 seemed to be a major nitrogen source during the stratified season at S1, but another nitrogen source is atmospheric nitrogen (N_2) fixation. At ALOHA, N_2 fixation contributes ~50% of the nitrogen for new production (Karl et al. 1997). On the basis of algological observations, symbiotic cyanobacteria (*Richelia* sp.), which are diazotrophs, were found in association with diatoms at S1 (Yamaguchi and Kawachi 2013). Such diatoms have occasionally been abundant during the summer at ALOHA (Villareal et al. 2011). However, it is unlikely that N_2 fixation is a major nitrogen source at S1 because microscopy and flow cytometry suggest that the population of diazotrophs at S1 is quite small compared with that of other phytoplankton throughout the year (Matsumoto et al. 2016). It is well known that N_2 fixation depends on Fe and phosphorus availability (Sohm et al. 2011). The very limited supply of both phosphate and nitrate during the stratified season at S1 (Wakita et al. 2016) would, therefore, restrict N_2 fixation.

In the summer of 2011, 18 profiling floats with a dissolved oxygen sensor were deployed around S1 to observe the spatial and temporal variability of the physical structure in this subtropical area and to study the interactions between physical oceanography and biogeochemistry. As a result, it was observed that in the following autumn, the concentration of oxygen increased in the subsurface layer (around 50 m) when a meso-scale eddy passed through the region (Inoue et al. 2016a; Kouketsu et al. 2016a). At that time, increases of subsurface Chl-*a* and organic carbon flux at 200 m were observed with the underwater profiling buoy system and time-series sediment trap (Inoue et al. 2016b). In addition, based on analysis of remotely sensed sea surface temperatures (SSTs), sea surface height anomaly (SSHA), and Chl-*a*, a positive association between the presence of a cyclonic eddy and Chl-*a* (Kouketsu et al. 2016b) and a negative correlation between SST and Chl-*a* (Siswanto et al. 2016a) were reported. These relationships suggest that a meso-scale eddy is one of the possible sources of nutrients at S1 and in subtropical regions. Sasai et al. (2010) simulated the effect of a cyclonic eddy on the marine ecosystem in the Kuroshio extension region. Oka and Qiu (2012) have reported that the stability of the Kuroshio extension impacts the frequency and magnitude of associated mesoscale eddies. The important role of eddies has previously been reported at the Bermuda-Atlantic Time Series (BATS) station in the subtropical North Atlantic. High biomass and primary productivity at the oligotrophic BATS site is partially maintained by episodic eddy-Ekman pumping (McGillicuddy et al. 1998).

Moreover, during the season when the ML is stratified, meteorological events such as storms and typhoons also thicken the ML, resulting in a supply of nutrients and an increase of phytoplankton (Babin et al. 2004; Toratani 2008; Siswanto et al. 2007, 2008; Shibano et al. 2011). Because climate change might alter the frequency and magnitude of typhoons in the future, continued time-series observations of meteorology, physical oceanography, and biogeochemistry in the subtropics will be required.

Another possible source of allochthonous nutrients is eolian inputs. It has been reported that eolian dust includes major and micro-nutrients (e.g., nitrogen and Fe, respectively), and terrestrial materials that enter the ocean affect ocean biogeochemistry (e.g., Jickells et al. 2005; Duce et al. 2008). During the 2013 summer cruise, only surface nutrient concentrations were elevated at S1. Nutrient concentrations below the surface to a depth of 100 m were depleted, and primary productivity was increased slightly compared to other summer cruises (MR13-04 Preliminary Cruise Report 2013). These observations may be evidence
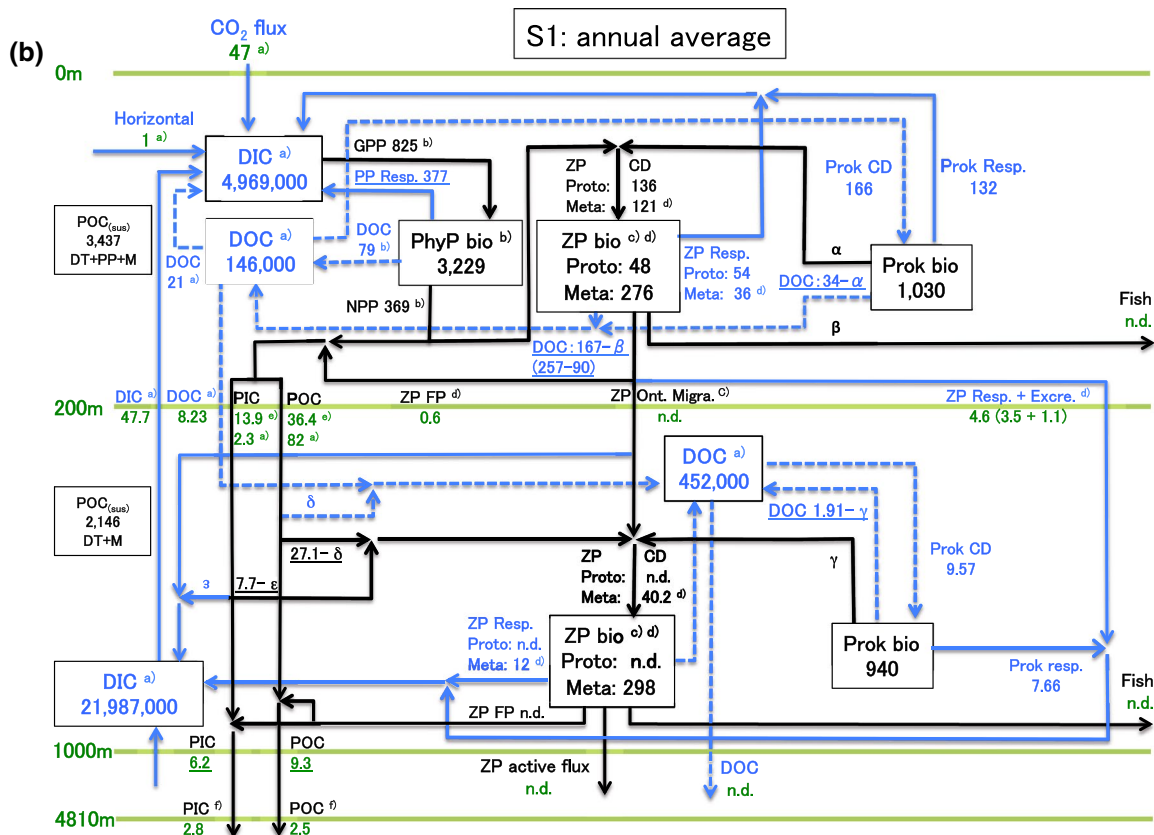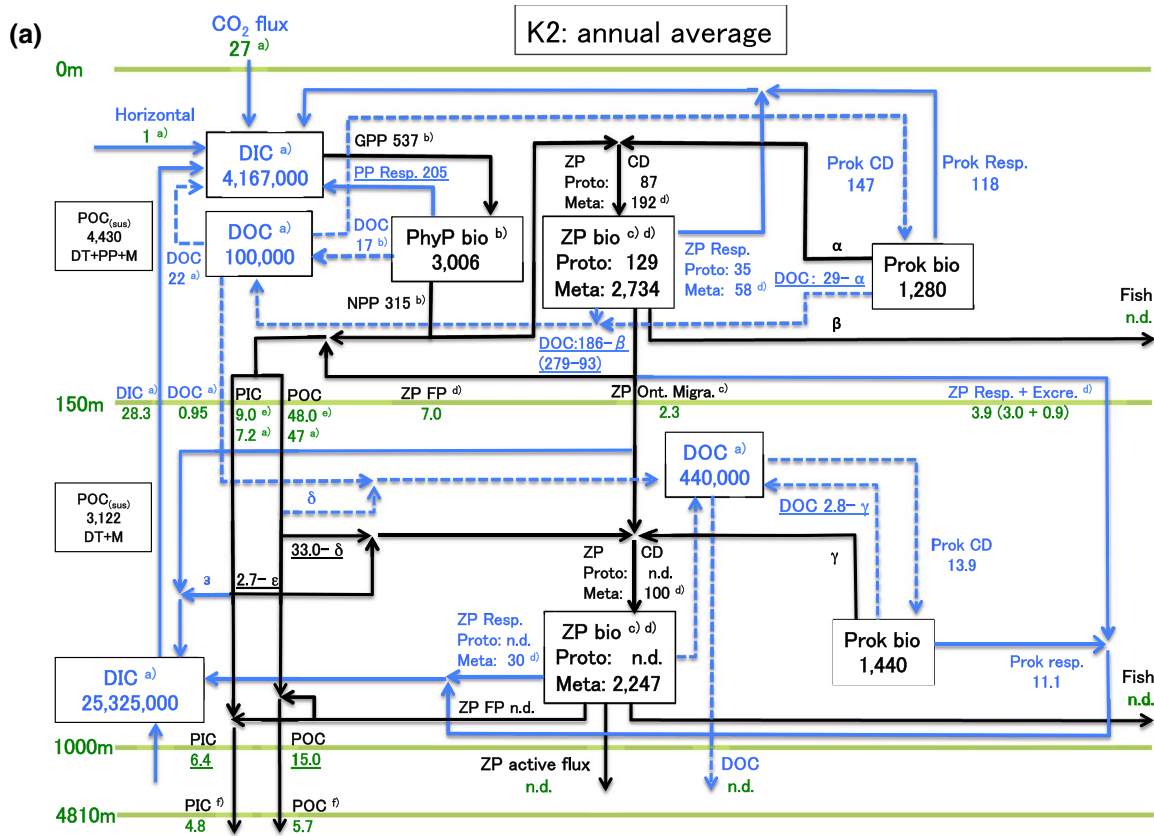
(a) K2: annual average

(b) S1: annual average

◀**Fig. 3** Carbon budget at **a** K2 and **b** S1. Abundances or reservoir sizes (*numbers in square*) are in mg-C m^{-2} and respective fluxes are in mg-C m^{-2} day^{-1}. Black (*blue*) numbers and lines are particulate (*dissolved*) phase. *Broken lines* are dissolved organic carbon (DOC). *Numbers in green* are flux at respective boundaries. Suspended substances, POC$_{(sus)}$ are regarded as the sum of detritus: DT, phytoplankton: PP, and heterotrophic microbes: M for the SML and sum of DT and M for the MPL. ZP is zooplankton. *Underlined numbers* are estimates based on respective budgets (see text). The n.d. means no data. "Proto" and "Meta" are protozoans (microzooplankton) and metazoans (mesozooplankton), respectively. CD, resp., and FP are carbon demand, respiration, and fecal pellet, respectively. Respective estimates are from the following papers: **a** Wakita et al. (2016), **b** Matsumoto et al. (2016), **c** Kobari et al. (2016), **d** Honda et al. (2016) and **e** K2S1 database. Note that some numbers do not match numbers in original papers because of the difference in target cruises and depths

of eolian nutrient inputs and their impact on primary productivity. In addition, during the K2S1 project, aerosols were collected onboard, and soluble Fe was measured. The results showed that aerosols smaller than 2.5 μm (PM$_{2.5}$) contained more soluble Fe than particles larger than 2.5 μm (F. Taketani, personal communication). The former and latter are likely anthropogenic and natural particles, respectively. The relatively large amount of soluble Fe in anthropogenic eolian dust has been previously reported (Sedwick et al. 2007; Baker and Croot 2008; Sholkovitz et al. 2009). Monitoring studies should therefore be undertaken to determine how an increase of eolian dust has an impact on ocean ecosystems and productivity in future.

4.3 Current status of ocean acidification

Carbonate chemistry has been monitored since 1997 at KNOT and since 2001 at K2. As a result, it has been statistically verified that the pH at the in situ temperature [pH$_{(in\ situ)}$], in winter ML has decreased, and this decrease has been accompanied by an increase of xCO$_2$ (CO$_2$ mol fraction in dry air) in the WSG (Fig. 4a). Below the ML, the pH$_{(in\ situ)}$ has decreased by a rate of 0.005 year^{-1}. In addition, the saturation depths for aragonite and calcite in 2011 were estimated to be ~115 and ~160 m, respectively (Fig. 4c), based on calculation with DIC and TALK data obtained during the K2S1 project and required constants (the carbonate dissociation constants: Mehrbach et al. 1973 as refitted by Dickson and Millero 1987, the thermodynamic solubility product constant: Mucci 1983). The saturation depth of calcite has shoaled at a rate of 3 m year^{-1} (Fig. 4c). These changes are thought to have been the result of increases of anthropogenic CO$_2$ uptake by the ocean and of the decomposition of organic materials evaluated from apparent oxygen usage (AOU: Wakita et al. 2010, 2013) caused by the increase of residence time of the intermediate water (Ono et al. 2001; Watanabe et al. 2001; Deutsh et al. 2005). The North Pacific

subarctic gyre has a low CaCO$_3$ saturation state (Ω) (e.g., Feely et al. 2009). The indication is, therefore, that future progression of ocean acidification would critically damage calcifiers. It is noted that saturation depth for aragonite did not show significant decrease trend unlike that for calcite at K2 (Fig. 4c). As shown in Fig. 4c, saturation depth for aragonite is located at around bottom of winter mixing layer (~110 m). On the other hand, xCO$_2$ (pH) in this layer show significant increase (decrease) trend (Fig, 4a). This is not incredible because, numerically, change rate of degree of saturation (Ω), that determines saturation depth of CaCO$_3$, is smaller than that of xCO$_2$ and pH (Egleston et al. 2010). In addition, change rate of Ω for aragonite [$\Omega_{(ara)}$] is smaller than that for calcite [$\Omega_{(cal)}$] on same isopycnic surface (Wakita et al. 2013). At K2, thickness of winter mixing layer varies inter-annually (~90–140 m: Wakita et al. 2013). It should introduce inter-annual variability in magnitude of vertical supply of subsurface water and/or horizontal supply of northern or southern water resulting in inter-annual variability in water temperature, salinity and carbonate system. Solubility constant (Ksp) for aragonite is more sensitive to change in temperature and salinity than Ksp for calcite (e.g. Sarmiento and Gruber 2006). Thus, larger inter-annual variability in $\Omega_{(ara)}$ might also hide significant decrease trend of saturation depth for aragonite. Contrast to saturation depth for aragonite, saturation depth for calcite is located subsurface layer (~160–200 m) where it is relatively more stable than the winter mixed layer from the viewpoint of physical oceanography and where, on the other hand, decomposition of organic materials occurs actively, resulting in a larger significant decrease in pH (Fig. 4a, c) and larger significant increase in DIC (Wakita et al. 2013) than in the winter mixing layer. Thus, the above points are likely reasons why saturation depth for aragonite did not show a significant decrease trend this study. In order to detect significant trend in carbonate system including ocean acidification near the upper ocean, more longer time-series observation at K2 is strongly recommended.

Of relevance to ocean acidification at S1 and throughout the western Pacific subtropical region is the fact that the estimated rate of decrease of pH$_{(in\ situ)}$ in the ML at S1 was 0.002 pH$_{(in\ situ)}$ year^{-1} (Fig. 4), which is similar to the rate estimated from previous observations near S1 (30°N, 137°E) (0.0018 pH$_{(in\ situ)}$ year^{-1}: JMA report, http://www.data.jma.go.jp/gmd/kaiyou/english/oa/oceanacidification_en.html, based on Midorikawa et al. 2010) and at ALOHA (0.0019 pH$_{(in\ situ)}$ year^{-1}: Dore et al. 2009), and faster than the rate at K2 (0.001 year^{-1}; Wakita et al. 2013) (Fig. 4a, b). Compared to the saturation depth for calcite in 2004 (~900 m; Feely et al. 2012), the rate of shoaling of the saturation depth between 2004 and 2011 was estimated to

Table 3 Comaparison of annual averages of carbon budget between K2 and S1

			K2	S1	Reference
= Surface mixed layer: SML (K2: 0 - 150 m, S1: 0 - 200 m) =					
CO_2 influx	(mg-C m^{-2} day^{-1})	*	27.3 ± 8.2	46.7 ± 14.1	Wakita et al. 2016
DIC abundance	(mg-C m^{-2})		4,167,000 ± 3,000	4,969,000 ± 4,000	Wakita et al. 2016
DIC entrainment from MPL	(mg-C m^{-2} day^{-1})	*	28.3 ± 0.3	47.7 ± 0.7	Wakita et al. 2016
DOC abundance	(mg-C m^{-2})	*	100,000 ± 1,000	146,000 ± 2,000	Wakita et al. 2016
DOC entrainment from MPL	(mg-C m^{-2} day^{-1})	*	0.95 ± 0.03	8.23 ± 0.33	Wakita et al. 2016
(= ~ DOC efflux from SML)					
POC(sus)	(mg-C m^{-2})	*	4,430 ± 343	3,437 ± 578	Kawakami et al. 2014
Phytoplankton					
Biomass	(mg-C m^{-2})		3,006 ± 595	3,229 ± 1,413	Matsumoto et al. 2014, 2016
Primary Productivity (PP)					
Gross PP	(mg-C m^{-2} day^{-1})	*	536 ± 106	825 ± 101	Matsumoto et al. 2014, 2016
Net PP	(mg-C m^{-2} day^{-1})		315 ± 39	369 ± 47	Matsumoto et al. 2014, 2016
DOC production	(mg-C m^{-2} day^{-1})	*	17 ± 2	79 ± 10	Matsumoto et al. 2014, 2016
Zooplankton					
Biomass					
Protozoan	(mg-C m^{-2})	*	129 ± 73	48 ± 11	This study
Metazoan	(mg-C m^{-2})	*	2,734 ± 1,370	276 ± 68	Kobari et al. 2016
Carbon demand					
Protozoan	(mg-C m^{-2} day^{-1})		87 ± 60	136 ± 28	This study
Metazoan	(mg-C m^{-2} day^{-1})		192 ± 62	121 ± 27	Kobari et al. 2016
Ontogenetic migration	(mg-C m^{-2} day^{-1})		2.3 ± 0.98	n.d.	This study
Fecal pellet flux	(mg-C m^{-2} day^{-1})	*	7.0 ± 2.0	0.6 ± 0.2	Kobari et al. 2016
Active carbon flux	(mg-C m^{-2} day^{-1})		3.9 ± 1.5	4.5 ± 1.1	
Prokaryote					
Biomass	(mg-C m^{-2})		1,280 ± 64	1,030 ± 52	This study
Carbon demand	(mg-C m^{-2} day^{-1})		147 ± 19	166 ± 22	This study
Sinking particle from SML					
POC flux			(150m)	(200m)	
by Drifting sediment trap	(mg-C m^{-2} day^{-1})	*	48.0 ± 4.8	36.4 ± 3.6	Honda et al. 2016
by Carbon balance	(mg-C m^{-2} day^{-1})	**	47 ± 14	82 ± 19	Wakita et al. 2016
PIC flux			(150m)	(200m)	
by Drifting sediment trap	(mg-C m^{-2} day^{-1})	*	9.0 ± 0.9	13.9 ± 1.4	Honda et al. 2016
by Carbon balance	(mg-C m^{-2} day^{-1})		7.2 ± 5.6	2.3 ± 7.6	Wakita et al. 2016
=Mesopelagic layer: MPL (K2: 150 - 1000 m, S1: 200 - 1000 m) =					
DIC abundance	(mg-C m^{-2})		25,325,000 ± 17,000	21,987,000 ± 17,000	Wakita et al. 2016
DOC abundance	(mg-C m^{-2})		440,000 ± 8,000	452,000 ± 8,000	Wakita et al. 2016
POC(sus)	(mg-C m^{-2})	*	3,122 ± 94	2,146 ± 64	Kawakami et al. 2014
Zooplankton					
Biomass					
Protozoan	(mg-C m^{-2})		n.d	n.d	
Metazoan	(mg-C m^{-2})	*	2,247 ± 159	298 ± 83.2	Kobari et al. 2016
Carbon demand					

Table 3 continued

			K2	S1	**Reference**
Protozoan	(mg-C m^{-2} day^{-1})		n.d	n.d	
Metazoan	(mg-C m^{-2} day^{-1})	*	100 ± 4	40 ± 11	Kobari et al. 2016
Prokaryote					
Biomass	(mg-C m^{-2})	*	1,440 ± 72	940 ± 47	This study
Carbon demand	(mg-C m^{-2} day^{-1})	*	13.9 ± 1.8	9.6 ± 1.2	This study
Sinking particle from MPL			(1000m)	(1000m)	
POC flux	(mg-C m^{-2} day^{-1})	*	15.0 ± 2.3	9.3 ± 1.4	This study
PIC flux	(mg-C m^{-2} day^{-1})		6.4 ± 1.0	6.2 ± 0.9	This study
=below 1000 m=					
Sinking particle at deep			(4810m)	(4810m)	
POC flux	(mg-C m^{-2} day^{-1})	*	5.7 ± 0.6	2.0 ± 0.2	K2S1 database (see URL in the text)
PIC flux	(mg-C m^{-2} day^{-1})	*	4.8 ± 0.5	2.8 ± 0.3	K2S1 database (see URL in the text)

Erros for respective budgets are measurement error or repeatability or standard deviation of seasonal variability (see Online Appendix 1)

* There is significant difference

** POC flux estimated based on carbon balance includes active carbon flux

be ~9 m year^{-1}, faster than the rate at K2 (~3 m year^{-1}) (Fig. 4c, d). These results are consistent with the fact that the western Pacific subtropical area, including S1, is a major anthropogenic CO_2 sink outside of the polar deep-water formation region (Sabine et al. 2004; Park et al. 2010). Although the Ω in the subtropical region is higher and the water is not corrosive for calcifiers at this moment, much attention should be paid to the rapid rate of acidification in this region.

4.4 Inter-annual variability and decadal change in biogeochemistry

Siswanto et al. (2015) conducted analysis of satellite-based estimates of SST, air temperature, wind velocity, Chl-*a*, and climatological data in the ML and revealed that, in the winter and autumn, the Pacific Decadal Oscillation Index (PDOI) and MLD were positively and negatively correlated in the northern area north of 42°N and southern area south of 42°N, respectively. They also found that the MLD was positively correlated with Chl-*a* in the southern part of the western North Pacific and negatively correlated with Chl-*a* in the northern part. Chiba et al. (2008) have also observed that deepening of the ML by the PDO was negatively correlated with Chl-*a* in the subarctic area. This correlation is likely caused by deepening of the ML in the subtropical area increases the nutrient supply and increases the Chl-*a*, whereas deepening of the ML

reduces the average PAR in the ML in the subarctic area, where nutrients are plentiful, even after autumn. Siswanto et al. (2016b) also conducted a trend analysis with sixteen-year-long satellite data. They revealed that a weak, but significant rising trend in sea surface temperature (SST) was responsible for the weak but significant Chl-*a* increasing trends in high latitudes (roughly north of 45°N) contrast to decreasing trend in the low latitudes (south of 45°N, east of 165°E). These observations thus indicate possible evidence that changes in meteorology and physical oceanography affect biogeochemistry differently in different locations.

5 Concluding remarks

Based on a seasonal comparative study, essential information about the ecosystem and cycling of materials was obtained in the subarctic and subtropical areas of the Northwestern Pacific. This information will aid predictions of how future climate/oceanic changes will affect the ecosystem and material cycles in the ocean. More studies were carried out as part of the K2S1 project including genetic analysis of bacteria (Kaneko et al., 2016) and regulation mechanisms of prokaryote production and respiration (Uchimiya et al. 2016) to elucidate microbial biodiversity, an analysis of nitrogen isotopes of sinking particles for the purpose of clarifying the
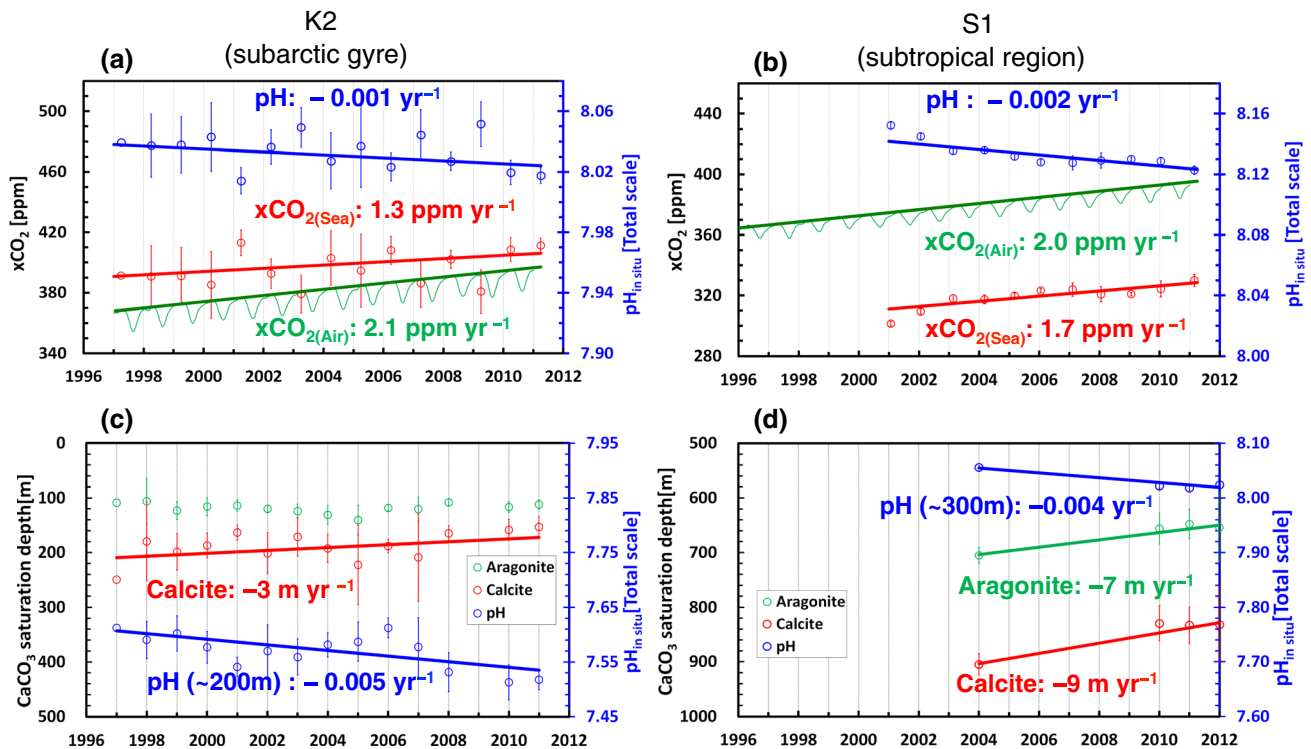
Fig. 4 Time-series of winter surface pH$_{(in\ situ)}$ (*blue circles*), xCO$_{2(sea)}$ in dry air and under 1 atmosphere and winter xCO$_{2(sea)}$ (mixing ratio of CO$_2$ by volume in dry air: *red circles*) at **a** K2 and **b** S1. *Green curves* in both figures show monthly average of xCO$_{2(air)}$ (Conway et al. 2012). *Lines* are statistically significant ($p < 0.05$) regression lines for respective winter data. **c** and **d** show subsurface pH (*blue circles*) and saturation depths of calcite (*red circles*) and aragonite (*green circles*) at K2 and S1, respectively. *Lines* are regression lines ($p < 0.05$) for respective data. **a** and **c** are modified from Figs. 3, 4 in Wakita et al. (2013). *Error bars* for respective data are standard devi-

ation. Surface pH$_{(in\ situ)}$ and xCO$_{2(sea)}$ in winter (January–March) at S1 were calculated by using TALK (Lee et al. 2006), fugacity of CO$_2$, which is pCO$_2$ corrected for non-ideal behavior of the gas (SOCAT version.2; Bakker et al. 2014) and required constants (Mehrbach et al. 1973; Mucci 1983; Dickson and Millero 1987). The CaCO$_3$ saturation depths for aragonite and calcite, and pH$_{(in\ situ)}$ at S1 were calculated from DIC and TALK data (2004: WOCE-P2 [http://cchdo.ucsd.edu/search?query=group%3Ap02]; 2010–2011: K2S1 project and Japan Meteorological Agency [http://www.data.jma.go.jp/gmd/kaiyou/db/vessel_obs/data-report/html/ship/ship.php])

nitrogen cycle (Mino et al. 2016), and a modeling study aimed at understanding the process of N$_2$O production (Yoshikawa et al. 2016).

References

Andreev A, Watanabe S (2002) Temporal changes in dissolved oxygen of the intermediate water in the subarctic North Pacific. Geophys Res Lett 29(14):1680. doi:10.1029/2002GL015021

Arrigo KR (2007) Carbon cycle: marine manipulation. Nature 450(22):491–492

Babin SM, Carton JA, Dickey TD, Wiggert JD (2004) Satellite evidence of hurricane-induced phytoplankton blooms in an oceanic desert. J Geophys Res 109:C03043. doi:10.1029/2003JC001938

Baker AR, Croot PL (2008) Atmospheric and marine controls on aerosol iron solubility in seawater. Mar Chem. doi:10.1016/j.marchem.2008.09.003

Bakker DCE, Pfeil B, Smith K, Hankin S, Olsen A, Alin SR, Cosca C, Harasawa S, Kozyr A, Nojiri Y, O'Brien KM, Schuster U, Telszewski M, Tilbrook B, Wada C, Akl J, Barbero L, Bates NR, Boutin J, Bozec Y, Cai WJ, Castle RD, Chavez FP, Che L, Chierici M, Currie K, De Baar HJW, Evans W, Feely RA, Fransson A, Gao Z, Hales B, Hardman-Mountford NJ, Hoppema M, Huang WJ, Hunt CW, Huss B, Ichikawa T, Johannessen T, Jones EM, Jones S, Jutterstrøm S, Kitidis V, Körtzinger A, Landschützer P, Lauvset SK, Lefèvre N, Manke AB, Mathis JT, Merlivat L, Metzl N, Murata A, Newberger T, Omar AM, Ono T, Park GH, Paterson K, Pierrot D, Ríos AF, Sabine CL, Saito S, Salisbury J, Sarma VVSS, Schlitzer R, Sieger R, Skjelvan I, Steinhoff T, Sullivan KF, Sun H, Sutton AJ, Suzuki T, Sweeney C, Takahashi T, Tjiputra J, Tsurushima N, Van Heuven SMAC, Vandemark D, Vlahos P, Wallace DWR, Wanninkhof R, Watson AJ (2014) An update to the Surface Ocean CO$_2$ Atlas (SOCAT version 2). Earth Syst Sci Data 6:69–90. doi:10.5194/essd-6-69-2014

Beherenfeld MJ, Falkowski PG (1997) A consumers guide to phytoplankton primary production models. Limnol Oceanogr 42:1479–1491

Bopp L, Monfray P, Aumont O, Dufresne J-L, Treut HL, Madec G, Terray L, Orr JC (2001) Potential impact of climate change on marine export production. Glob Biogeochem Cycles 15:81–99

Bopp L, Aumont O, Cadule P, Alvain S, Gehlen M (2005) Response of diatoms distribution to global warming and potential implications: a global model study. Geophys Res Lett 32:L19606. doi:10.1029/2005GL023653

Bopp L, Resplandy Orr JC, Doney SC, Dunne JP, Gehlen M, Halloran P, Heinze C, Ilyina T, Seferian R, Tjiputra J, Vichi M (2013) Multiple stressors of ocean ecosystems in the 21st century: projections with CMIP5 models. Biogeosci 10:6115–6245. doi:10.5194/bg-10-6225-2013

Boyd PW, Lennartz ST, Glover DM, Doney SC (2015) Biological ramifications of climate-change-mediated oceanic multi-stressors. Nature climate change 5:71–79. doi:10.1038/NCLIMATE2441

Buesseler KO, Lamborg CH, Boyd PW, Lam PJ, Trull TW, Bidigare RR, Bishop JKB, Casciotti KL, Dehairs F, Elskens M, Honda MC, Karl DM, Siegel DA, Silver MW, Steinberg DK, Valdes J, Mooy BV, Wilson S (2007) Revisiting carbon flux through the ocean's twilight zone. Science 316:567–570

Buesseler KO, Trull TW, Steinberg DK, Silver MW, Siegel DA, Saitoh S, Lamborg CH, Lam PJ, Karl DM, Jiao NZ, Honda MC, Elskens M, Dehairs F, Brown SL, Boyd PW, Bishop JKB, Bidigare RR (2008) VERTIGO (VERtical Transport In the Global Ocean): a study of particle sources and flux attenuation in the North Pacific. Deep-Sea Res 55(14–15):1522–1539

Caron DA, Goldman JC (1990) Protozoan nutrient regeneration. In: Capriulo GM (ed) Ecology of marine protozoa. Oxford University Press, New York, pp 283–306

Chiba S, Aita MN, Tadokoro K, Saino T, Sugisaki H, Nakata K (2008) From climate regime shift to lower-tropic level phenology: synthesis of recent progress in retrospective studies of the Western North Pacific. Progress Oceanogr 77:112–126. doi:10.1016/j.pocean.2008.03.004

Conway TJ, Masarie KA, Lang PM, Tans PP (2012) NOAA Greenhouse Gas Reference from Atmospheric Carbon Dioxide Dry Air Mole Fractions from the NOAA ESRL Carbon Cycle Cooperative Global Air Sampling Network Path: ftp://ftp.cmdl.noaa.gov/ccg/co2/flask/

del Giorge PA, Cole JJ (2000) Bacteria energetics and growth efficiency. In: Kirchman DL (ed) Microbial ecology of the oceans, Wiley-Liss, Hoboken, vol 99, pp 289–325

Denman KL, Pena MA (2002) The response of two coupled one-dimensional mixed layer/plankton ecosystem models to climate change in the NE subarctic Pacific Ocean. Deep Sea Res II 49:5739–5758

Deutsh C, Emerson S, Thompson L (2005) Fingerprints of climate change in North Pacific oxygen. Geophys Res Lett 32:L16604. doi:10.1029/2005GL023190

Dickson AG, Millero FJ (1987) A comparison of the equilibrium constants for the dissociation of carbonic acid in seawater media. Deep Sea Res Part A 34:1733–1743

Dlugokency EJ, Masarie KA, Lang PM, Tans PP (2014) NOAA Greenhouse Gas Reference from Atmospheric Carbon Dioxide Dry Air Mole Fractions from the NOAA ESRL Carbon Cycle Cooperative Global Air Sampling Network. Data Path: http://a.cmdl.noaa.gov/data/trace_gases/co2/flask/surface/

Doney SC (2006) Plankton in a warmer world. Nature 444:695–696

Dore JE, Lukas Sadler RDW, Church MJ, Karl DM (2009) Physical and biogeochemical modulation of ocean acidification in the central North Pacific. Proc Natl Acad Sci USA 106:12235–12240

Duce RA, LaRoche J, Altieri K, Arrigo KR, Baker AR, Capone DG, Cornell S, Dentener F, Galloway J, Ganeshram RS, Geider RJ, Jickells T, Kuypers MM, Langlois R, Liss PS, Liu SM, Middelburg JJ, Moore CM, Nickovic S, Oschlies A, Pedersen T, Prospero J, Schlitzer R, Seitzinger S, Sorensen LL, Uematsu M, Ulloa O, Voss M, Ward B, Zamora L (2008) Impacts of atmospheric anthropogenic nitrogen on the open ocean. Science 320:893–897

Egleston ES, Sabine CL, Morel FMM (2010) Revelle revisited: Buffer factors that quantify the response of ocean chemistry to changes in DIC and alkalinity. Global Biogeochem Cycles 24: GB1002 doi:10.1029/2008GB003407

Feely RA, Doney SC, Cooley SR (2009) Ocean acidification. Oceangr 22(4):36–47

Feely RA, Sabine CL, Byrne RH, Millero FJ, Dickson AG, Wanninkhof R, Murata A, Miller LA (2012) Decadal changes in the aragonite and calcite saturation state of the Pacific Ocean. Global Biogeochem Cycles. GB3001. doi:10.1029/2011GB004157

Fenchel T, Finlay BJ (1983) Respiration rates in heterotrophic free-living protozoa. Microb Ecol 9:99–122

Fujiki T, Matsumoto K, Mino Y, Sasaoka K, Wakita M, Kawakami H, Honda MC, Watanabe S, Saino T (2014) The seasonal cycle of phytoplankton community structure and photophysiological state in the western subarctic gyre of the North Pacific. Limnol Oceanogr 59(3):887–900

Fukuda H, Ogawa H, Nagata T, Koike I (1998) Direct determination of carbon and nitrogen contents of natural bacterial assemblages in marine environments. Appl Environ Microbiol 64(9):3352–3358

Giering SLC, Sanders R, Lampitt RS, Anderson TR, Tamburini C, Boutrif M, Zubkov MV, Marsay CM, Henson SA, Saw K, Cook K, Mayor DJ (2014) Reconciliation of the carbon budget in the ocean's twilight zone. Nature 507:480–483. doi:10.1038/nature13123

Gnaiger E (1983) Calculation of energetic and biochemical equivalents of respiratory oxygen consumption. In: Gnaiger E, Forster H (eds) Polar organic oxugen sensors. Springer, Berlin, pp 337–345

Gregg WW, Ginoux P, O'Reilly JE, Casey NW (2003) Ocean primary production and climate: Global decadal changes. Geophys Res Lett 30 (15). doi:10.1029/2003GL016889

Harrison PJ, Boyd PW, Varela DE, Takeda S, Shiomoto A, Odate T (1999) Comparison of factors controlling phytoplankton productivity in the NE and NW Subarctic Pacific Gyres. Prog Oceanogr 43:205–234

Harrison PJ, Whitney FA, Tsuda A, Saito H, Tadokoro K (2004) Nutrient and plankton dynamics in the NE and NW gyres of the subarctic Pacific Ocean. J Oceanogr 60:93–117

Hashioka T, Sakamoto TT, Yamanaka Y (2009) Potential impact of global warming on North Pacific spring blooms projected by an eddy-permitting 3-D ocean ecosystem model. Geophys Res Lett 36:L20604. doi:10.1029/2009GL038912

Heinze C (2004) Simulating oceanic CaCO$_3$ export production in the greenhouse. Geophys Res Lett 31:L16308. doi:10.1029/2004GL020613

Honda MC (2003) Biological pump in the northwestern North Pacific. J Oceanogr 59:671–684

Honda MC, Watanabe S (2007) Utility of an automatic water sampler to observe seasonal variability in nutrients and DIC in the Northwestern North Pacific. J Oceanogr 63:349–362

Honda MC, Watanabe S (2010) Importance of biogenic opal as ballast of particulate organic carbon (POC) transport and existence of mineral ballast-associated and residual POC in the Western Pacific Subarctic Gyre. Geophys Res Lett 37:L02605. doi:10.1029/2009GL041521

Honda MC, Imai K, Nojiri Y, Hoshi F, Sugawara T, Kusakabe M (2002) The biological pump in the northwestern North Pacific based on fluxes and major components of particulate matter obtained by sediment trap experiments (1997-2000). Deep-Sea Res II 49:5595–5626

Honda MC, Kawakami H, Sasaoka K, Watanabe S, Dickey T (2006) Quick transport of primary produced organic carbon to the ocean interior. Geophys Res Lett 33: doi:10.1029/2006GL026466

Honda MC, Sasaoka K, Kawakami H, Matsumoto K, Watanabe S, Dickey TD (2009) Application of underwater optical data to estimation of primary productivity. Deep Sea Res I 56:2281–2292

Honda MC, Kawakami H, Watanabe S, Saino T (2013) Concentration and vertical flux of Fukushima-derived radiocesium in sinking particles from two sites in the Northwestern Pacific Ocean. Biogeosciences 10:3525–3534. doi:10.5194/bg-10-3525-2013

Honda MC, Kawakami H, Matsumoto K, Wakita M, Fujiki T, Mino Y, Sukigara C, Kobari T, Uchimiya M, Kaneko R, Saino T (2016) Comparison of sinking particles in the upper 200 m between subarctic station K2 and subtropical station S1 based on drifting sediment trap experiments. J Oceanogr 72:373–386. doi:10.1007/s10872-015-0280-x

Hosoda S, Ohira T, Sato K, Suga T (2010) Improved description of global mixed-layer depth using Argo profiling floats. J Oceanogr 66:773–787. doi:10.1007/s10872-010-0063-3

Imai K, Nojiri Y, Tsurushima N, Saino T (2002) Time series of seasonal variation of primary productivity at station KNOT (44°N, 155°E) in the sub-arctic western North Pacific. Deep Sea Res II 49:5395–5408

Inoue R, Suga T, Kouketsu S, Hosoda S, Kobayashi T, Sato K, Nakajima H, Kawano T (2016a) Western North Pacific Integrated Physical-Biogeochemical Ocean Observation Experiment (INBOX): part 1. Specifications and Chronology of the S1-INBOX floats. J Mar Res 74:43–69

Inoue R, Honda MC, Fujiki T, Matsumoto K, Kouketsu S, Suga T, Saino T (2016b) Western North Pacific Integrated Physical-Biogeochemical Ocean Observation Experiment (INBOX): part 2. Biogeochemical responses to eddies and typhoons revealed from shipboard measurements and the S1 biogeochemical moorings during S1-INBOX. J Mar Res 74:71–99

IPCC (2013) Climate change 2013: The physical science basis. In: Stocker TF, Qin D, Plattner GK, Tignor M, Allen SK, Boschung J, Nauels A, Xia Y, Bex V, Midgley PM (eds) Contribution of working group I to the fifth assessment report of the Intergovernmental Panel on Climate Change. Cambridge University Press, Cambridge, p 1535

Ishida H, Watanabe YW, Ishizaka J, Nakano T, Nagai N, Watanabe Y, Shimamoto A, Maeda N, Magi M (2009) Possibility of recent changes in vertical distribution and size composition of chlorophyll-a in the western North Pacific region. J Oceanogr 65:179–186

Jickells TD, An ZS, Andersen KK, Baker AR, Bergametti G, Brooks N, Cao JJ, Boyd PW, Duce RA, Hunter KA, Kawahata H, Kubilay N, laRoche J, Liss PS, Mahowald N, Prospero JM, Ridgwell AJ, Tegen STorres R, Torres R (2005) Global iron connections between desert dust, Ocean biogeochemistry, and climate. Science 308:67–71

JMA: Japan Meteorological Agency (2008) Annual report on atmospheric and marine environment monitoring No. 8, Observation Results for 2006 [CD-ROM], Tokyo

Kaneko R, Suzuki S, Nagata T, Hamasaki K (2016) Depth-dependent (0–5000 m) and seasonal variability in archaeal community structure in the subarctic and subtropical North Pacific Ocean. J Oceanogr 72:427–438. doi:10.1007/s10872-016-0372-2

Karl DM, Christian JR, Dore JE, Hebel DV, Letelier RM et al (1996) Seasonal and interannual variability in primary production and particle flux at station Aloha. Deep-Sea Res II 43:539–568

Karl DM, Letelier R, Tupas L, Dore J, Christian J, Hebel D (1997) The role of nitrogen fixation in biogeochemical cycling in the subtropical North pacific Ocean. Nature 388:533–538

Karl DM, Michaels AF, Bates NR, Knap A (2001) Building the long-term picture: the U.S.JGOFS time-series programs. Oceanography 14(4):6–17

Kawakami H, Honda MC (2007) Time-series observation of POC fluxes estimated from ^{234}Th in the northwestern North Pacific. Deep Sea Res I 54:1070–1090

Kawakami H, Honda MC, Wakita M, Watanabe S (2007) Time-series observation of dissolved inorganic carbon and nurients in the northwestern North Pacific. J Oceanogr 63:967–982

Kawakami H, Honda MC, Watanabe S, Saino T (2014) Time-series observations of ^{210}Po and ^{210}Pb radioactivity in the western North Pacific. J Radioanal Nucl Chem. doi:10.1007/s10967-014-3141-y

Kawakami H, Honda MC, Matsumoto K, Wakita M, Kitamura M, Fujiki T, Watanabe S (2015) POC fluxes estimated from ^{234}Th in late spring-early summer in the western subarctic North Pacific. J Oceanogr 71:311–324. doi:10.1007/s10872-015-0290-8

Kitamura M, Kobari T, Honda MC, Matsumoto K, Sasaoka K, Nakamura R, Tanabe K (2016) Seasonal changes of mesozooplankton biomass and community structure in the subarctic and subtropical time-series stations in the western North Pacific. J Oceanogr 72:387–402. doi:10.1007/s10872-015-0347-8

Kobari T, Shinada A, Tsuda A (2003) Functional roles of interzonal migrating mesozooplankton in the western subarctic Pacific. Prog Oceanogr 57:279–298

Kobari T, Steinberg DK, Ueda A, Tsuda A, Silver MW, Kitamura M (2008) Impacts of ontogenetically migrating copepods on downward carbon flux in the western subarctic Pacific Ocean. Deep Sea Res II 55:1648–1660

Kobari T, Kitamura M, Minowa M, Isami H, Akamatsu H, Kawakami H, Matsumoto K, Wakita M, Honda MC (2013) Impacts of the wintertime mesozooplankton community to downward carbon flux in the subarctic and subtropical Pacific Oceans. Deep Sea Res I 81:78–88

Kobari T, Nakamura R, Unno K, Kitamura M, Tanabe K, NAgafuku H, Niibo A, Kawakami H, Matsumoto K, Honda MC (2016) Seasonal variability of carbon demands and fluxes by mesozooplankton community at subarctic and subtropical sites in the western North Pacific. J Oceanogr 72:403–418. doi:10.1007/s10872-015-0348-7

Kouketsu S, Inoue R, Suga T (2016a) Western North Pacific Integrated physical-biogeochemical ocean observation experiment (INBOX): part 3. Mesoscale variability of dissolved oxygen concentrations observed by multiple floats during S1-INBOX. J Mar Res 74:101–131

Kouketsu S, Kaneko H, Okunishi T, Sasaoka K, Itoh S, Inoue R, Ueno H (2016b) Mesoscale eddy effects on temporal variability of surface chlorophyll a in the Kuroshio Extension. J Oceanogr 72:439–451. doi:10.1007/s10872-015-0286-4

Kwon EY, Primeau F, Sarmiento JL (2009) The impact of remineralization depth on the air-sea carbon balance. Nat Geosci 2:630–635

Laws EA, Falkowski PG, Smith WO Jr, Ducklow H, McCarthy JJ (2000) Temperature effects on export production in the open ocean. Glob Baiogeochem Cycles 14:1231–1246

Lee K, Tong LT, Millero FJ, Sabine CL, Dickson AG, Goyet C, Park GH, Wanninkhof R, Feely RA, Key RM (2006) Global relationships of total alkalinity with salinity and temperature in surface

waters of the world's oceans. Geophys Res Lett 33:L19605. doi :10.1029/2006GL027207

Letelier RM, Dore JE, Winn CD, Karl DM (1996) Seasonal and inter-annual variations in photosynthetic carbon assimilation at station ALOHA. Deep Sea Res II 43(2–3):467–490

Limsakul A, Saino T, Goes JI, Midorikawa T (2002) Seasonal variability in the lower trophic level environments of the western subtropical Pacific and Oyashio waters – A retrospective study. Deep Sea Res II 49:5487–5512. doi:10.1016/S0967-06445(02)00208-4

Liu H, Imai K, Suzuki K, Nojiri Y, Tsurushima N, Saino T (2002) Seasonal valiability of picophytoplankton and bacteria in the western subarctic Pacific Ocean at station KNOT. Deep Sea Res 49:5409–5420

Mantua NJ, Hare SR, Zhang Y, Wallace JM, Francic RC (1997) A Pacific interdecadal climate oscillation with impacts on salmon production. Bull Am Meteorol Soc 78:1069–1079

Martin JH, Knauer GG, Karl DM, Broenkow WW (1987) VERTEX: carbon cycling in the northeast Pacific. Deep Sea Res 34:267–285

Matsumoto K, Honda MC, Sasaoka K, Wakita M, Kawakami H, Watanabe S (2014) Seasonal variability of primary production and phytoplankton biomass in the western Pacific subarctic gyre: control by light availability within the mixed layer. J Geophys Res Oceans 119(9):6523–6534. doi:10.1002/2014JC009982

Matsumoto K, Abe O, Fujiki T, Sukigara C, Mino Y (2016) Primary productivity at the time-series stations in the northwestern Pacific Ocean: is the subtropical station unproductive? J Oceanogr 72:359–371. doi:10.1007/s10872-016-0354-4

McGillicuddy DJ, Robinson AR, Siegel DA, Jannasch HW, Johnson R, Dickey TD, McNeil J, Michaels AF, Knap AH (1998) Influence of mesoscale eddies on new production in the Sargasso Sea. Nature 394(6690):263–266

Mehrbach C, Culberson CH, Hawley JE, Pytkowicz RM (1973) Measurement of the apparent dissociation constants of carbonic acid in seawater at atmospheric pressure. Limnol Oceanogr 18:897–907

Midorikawa T, Ishii M, Saito S, Sasano D, Kosugi N, Motoi T, Kamiya H, Nakadate A, Nemoto K, Inoue HY (2010) Decreasing pH trend estimated from 25-yr time series of carbonate parameters in the western North Pacific. Tellus B 62:649–659. doi:10.1111/j.1600-0889.2010.00474.x

Mino Y, Sukigara C, Kawakami H, Honda MC, Matsumoto K, Wakita M, Kitamura M, Fujiki T, Sasaoka K, Abe O, Kaiser J, Saino T (2016) Seasonal variations in the nitrogen isotopic composition of settling particles at station K2 in the western subarctic North Pacific. J Oceanogr. doi:10.1007/s10872-016-0381-1

Mochizuki M, Shiga N, Saito M, Imai K, Nojiri Y (2002) Seasonal changes in nutrients, chlorophyll a and phytoplankton assemblage of the western subarctic gyre in the Pacific Ocean. Deep Sea Res 49:5421–5440

Moran XAG, Lopez-Urrutia A, Calvo-Diaz A, Li WKW (2010) Increasing importance of small phytoplankton in the warmer ocean. Glob Change Biol 16:1137–1144. doi:10.1111/j.1365-2486.2009.01960.x

MR13-04 Preliminary cruise report (2013) http://www.godac.jam-stec.go.jp/catalog/data/doc_catalog/media/MR13-04_all.pdf. Accessed 3 Apr 2017

Mucci A (1983) The solubility of calcite and aragonite in sea water at various salinities, temperatures and one atmosphere total pressure. Am J Sci 238:780–799

Ogawa H, Usui T, Koike I (2003) Distribution of dissolved organic carbon in the East China Sea. Deep Sea Res II 50:353–366

Oka E, Qiu B (2012) Progress of North Pacific mode water research in the past decade. J Oceanogr 68:5–20

Ono T, Midorikawa T, Watanabe YW, Tadokoro K, Saino T (2001) Temporal increases of phosphate and apparent oxygen utilization in the subsurface waters of western subarctic Pacific from 1968 and 1998. Geophys Res Lett 28:3285–3288

Ono T, Tadokoro K, Midorikawa T, Nishioka J, Saino T (2002) Multi-decadal decrease of net community produc-tion in western subarctic North Pacific. Geophys Res Lett. doi:10.1029/2001GL014332

Park GH, Wanninkhof R, Doney SC, Takahashi T, Lee K, Feely RA, Sabine CL, Trinanes J (2010) Variability of global net sea-air CO2 fluxes over the last three decades using empirical relationships. Tellus 62B:352–368

Pierrot DEL, Wallace DWR (2006) MS Excel program developed for CO_2 System Calculations, ORNL/CDIAC-105, Oak Ridge, Tennessee, Carbon Dioxide Information Analysis Center, Oak Ridge National Laboratory, US Department of Energy

Reid JLJr (1965) Intermediate waters of the Pacific Ocean. The Johns Hopkins Oceanographic Studies 2, p 85

Sabine CL, Feely RA, Gruber N, Key RM, Lee K, Bullister JL, Wanninkhof R, Wong CS, Wallace DWR, Rilbrook B, Millero FJ, Peng TH, Kozyr A, Ono T, Aida FR (2004) The oceanic sink for anthropogenic CO_2. Science 305:367–371

Saino T, Bychkov A, Chen CTA, Harrison PJ (2002) The joint global ocean flux study in the North Pacific. Deep Sea Res II 49:5297–5301

Sarmiento JL, Gruber N (2006) Ocean biogeochemical dynamics. Princeton University Press, New Jersey, p 503

Sasai Y, Richards KJ, Ishida A, Sasaki H (2010) Effects of cyclonic mesoscale eddies on the marine ecosystem in the Kuroshio Extension region using an eddy-resolving coupled physical-biological model. Ocean Dyn 60(3):693–704. doi:10.1007/s10236-010-0264-8

Sasai Y, Yoshikawa C, Smith SL, Hashioka T, Matsumoto K, Wakita M, Sasaoka K, Honda MC (2016) Coupled 1-D physical-biological model study of phytoplankton production at two contrasting time series stations in the western North Pacific. J Oceanogr 72:509–526. doi:10.1007/s10872-015-0341-1

Sathyendranath S, Stuart V, Nair A, Oka K, Nakane T, Bouman H, Forget MH, Maass H, Platt T (2009) Carbon-to-chlorophyll ratio and growth rate of phytoplankton in the sea. Mar Ecol Prog Seri 383:73–84

Sedwick PN, Sholkovitz ER, Church TM (2007) Impact of anthro-pogenic combustion emissions on the fractional solubility of aerosol iron: evidence from Sargasso Sea. Geochem Geophys Geosys 8: Q10Q06. doi:10.1029/2007GC001586

Shibano R, Yamanaka Y, Okada N, Chuda T, Suzuki S, Niino H, Toratani M (2011) Responses of marine ecosystem to typhoon passages in the western subtropical North Pacific. Geophys Res Lett 38:L18608. doi:10.1029/2011GL048717

Sholkovitz ER, Sedwick PN, Church TM (2009) Influence of anthro-pogenic combustion emissions on the deposition of soluble aerosol iron to the ocean: empirical estimates for island sites in the North Atlantic. Geochim Cosmochim Acta 73:3981–4003. doi:10.1016/j.gca.2009.04.029

Siswanto E, Ishizaka J, Yokouchi K, Tanaka K, Tan CK (2007) Estimation of interannual and interdecadal variations of typhoon-induced primary production: a case study for the outer shelf of the East China Sea. Geophys Res Lett 34:L03604. doi:10.1029/2006GL028368

Siswanto E, Ishizaka J, Morimoto A, Tanaka K, Okamura K, Kristijono A, Saino T (2008) Ocean physical and biogeochemical responses to the passage of typhoon Meari in the East China Sea observed from Argo float and multiplatform satellites. Geophys Res Lett 35:L15604. doi:10.1029/2008GL035040

Siswanto E, Matsumoto K, Fujiki T, Honda MC, Sasaoka K, Saino T (2015) Reappraisal of meridional differences of factors

controlling phytoplankton biomass and initial increase preceding seasonal Bloom in the Northwestern Pacific Ocean. Remote Sens Environ 159:44–56

Siswanto E, Honda MC, Sasai Y, Sasaoka K, Saino T (2016a) Meridional and seasonal footprints of the Pacific Decadal Oscillation on phytoplankton biomass in the northwestern Pacific Ocean. J Oceanogr 72:465–477. doi:10.1007/s10872-016-0367-z

Siswanto E, Honda MC, Matsumoto K, Sasai Y, Fujiki T, Sasaoka K, Saino T (2016b) Sixteen-year phytoplankton biomass trend in the northwestern Pacific Ocean observed by the SeaWiFS and MODIS ocean color sensors. J Oceanogr 72:479–489. doi:10.1007/s180872-016-0357-1

Smith SL (2011) Consistently modeling the combined effects of temperature and concentration on nitrate uptake in the ocean. J Geophys Res Biogeosci 116:G04020. doi:10.1029/2011JG001681

Sohm JA, Webb EA, Capone DG (2011) Emerging patterns of marine nitrogen fixation. Nat Rev Microbiol 9:499–508

Steinberg DK, Cope JS, Wilson SE, Kobari T (2008a) A comparison of mesopelagic mesozooplankton community structure in the subtropical and subarctic North Pacific Ocean. Deep Sea Res II 55:1615–1635

Steinberg DK, Van Mooy BAS, Buesseler KO, Boyd PW, Kobari T, Karl D (2008b) Bacteria vs. zooplankton control of sinking particle flux in the ocean's twilight zone. Limnol Oceanogr 53:1327–1338

Suga T, Hanawa K (1990) The mixed layer climatology in the northwestern part of the North Pacific subtropical gyre and the formation area of Subtropical Mode Water. J Mar Res 48:543–566

Timothy DA, Wong SC, Barwell-Clarke JE, Page JS, White LA, Macdonald RW (2013) Climatology of sediment flux and composition in the subarctic Northeast pacific Ocean with biogeochemical implications. Progr Oceanogr 116:95–129

Toratani M (2008) Primary production enhancement by typhoon Ketsana in 2003 in western North Pacific. SPIE Remote Sens Inland Coast Ocean. Waters. 7150. doi: 10.1117/12806426

Tsuda A, Takeda S, Saito H, Nishioka J, Nojiri Y, Kudo I, Kiyosawa H, Shiomoto A, Imai K, Ono T, Shimamoto A, Tsumune D, Yoshimura T, Aono T, Hinuma A, Kinugasa M, Suzuki K, Sohrin Y, Noiri Y, Tani H, Deguchi Y, Tsurushima N, Ogawa H, Fukami K, Kumaand K, Saino T (2003) A mesoscale iron enrichment in thewestern subarctic pacific induces large centric diatombloom. Science 300:958–961

Tsurushima N, Nojiri Y, Imai K, Watanabe S (2002) Seasonal variations of carbon dioxide system and nutrients in the surface mixed layer at station KNOT (44°N, 155°E) in the subarctic western North Pacific. Deep Sea Res II 49:5377–5394

Uchimiya M, Ogawa H, Nagata T (2016) Effects of temperature elevation and glucose addition on prokaryotic production and respiration in the mesopelagic layer of the western North Pacific. J Oceanogr 72:419–426. doi:10.1007/s10872-015-0294-4

Uda M (1963) Oceanography of the subarctic Pacific Ocean. J Fish Res Board Can 20:119–179

Villareal TA, Adornato L, Wilson C, Schoenbaechler CA (2011) Summer blooms of diatom-diazotroph assemblages and surface chlorophyll in the North Pacific gyre: a disconnect. J Geophys Res: Oceans 116(C3):C03001. doi:10.1029/2010JC006268

Volk T, Hoffert MI (1985) Ocean carbon pumps: Analysis of relative strengths and efficiencies in ocean-driven atmospheric CO_2 changes. In: Sundquist ET, Broecker WS (eds) The carbon cycle and atmospheric CO_2: natural variations archean to present, 32. Geophysical Monograph, American Geophysical Union, Washington, pp 99–110

Wakita M, Watanabe S, Murata A, Tsurushima N, Honda MC (2010) Decadal change of dissolved inorganic carbon in the subarctic western North Pacific Ocean. Tellus B 62:608–620. doi:10.1111/j.1600-0889.2010.00476.x

Wakita M, Watanabe S, Honda MC, Nagano A, Kimoto K, Matsumoto K, Kawakami H, Fujiki T, Kitamura M, Sasaki K, Sasaoka K, Nakano Y, Murata A (2013) Ocean acidification from 1997 to 2011 in the subarctic western North Pacific Ocean. Biogeosciences 10:7817–7827. doi:10.5194/bg-10-7817-2013

Wakita M, Honda MC, Matsumoto K, Fujiki T, Kawakami H, Yasunaka S, Sasai Y, Sukigara C, Uchimiya M, Kitamura M, Mino Y, Nagano A, Usui N, Watanabe S, Saino T (2016) Biological organic carbon export estimated from carbon budget in the surface water of western subarctic and subtropical North Pacific Ocean. J Oceanogr 72:665–685. doi:10.1007/s10872-016-0379-8

Watanabe YW, Ono T, Shimamoto A, Sugimoto T, Wakita M, Watanabe S (2001) Probability of a reduction in the formation rate of the subsurface water in the North Pacific during the 1980s and 1990s. Geophys Res Lett 28:3289–3292

Watanabe YW, Shigemitsu M, Tadokoro K (2008) Evidence of a change in oceanic fixed nitrogen with decadal climate change in the North Pacific subpolar region. Geophys Res Lett 35:L01602. doi:10.1029/2007GL032188

Watanabe YW, Shigemitsu M, Ujiie T, Minami H (2014) Decadal shift of biogenic sinking particle flux in the western North Pacific subpolar region. Geophys Res Lett 41(2):513–518. doi:10.1002/2013GL059142

Wilson S, Steinberg DK, Buesseler K (2008) Changes in fecal pellet characteristics with depth as indicators of zooplankton repackaging of particles in the mesopelagic zone of the subtropical and subarctic North Pacific Ocean. Deep Sea Res II 55:1636–1647

Winn CD, Mackenzie FT, Carrillo CJ, Sabine CL, Karl DM (1994) Air-sea carbon dioxide exchange in the North Pacific Subtropical Gyre: implications for the global carbon budget. Glob Biogeochem Cycles 8(2):157–163

Wong CS, Chan YH (1991) Temporal variations in the partial pressure and flux of CO_2 at ocean station P in the subarctic northeast Pacific Ocean. Tellus 43B:206–223

Wong CS, Waser NAD, Nojiri Y, Whitney FA, Page JS, Zeng J (2002a) Seasonal cycles of nutrients and dissolved inorganic carbon at high and mid latitudes in the North Pacific Ocean during *Skaugran* cruises: determination of new production and nutrient uptake ratios. Deep-Sea Res II 49:5317–5338

Wong CS, Waser NAD, Whitney FA, Johnson WK, Page JS (2002b) Time-series study of the biogeochemistry of the North East subarctic Pacific: reconciliation of the Corg/N remineralization and uptake ratios with the Redfield ratios. Deep Sea Res II 49:5717–5738

Yamaguchi H, Kawachi M (2013) Taxonomy and genome analysis of eukaryotic picophytoplankton originated from cryopreserved narine environmental specimens MR13-04 Preliminary Cruise Report, p 125–138. http://www.godac.jamstec.go.jp/catalog/data/doc_catalog/media/MR13-04_all.pdf. Accessed 3 Apr 2017

Yamaguchi A, Watanabe Y, Ishida H, Harimoto T, Furusawa K, Suzuki S, Ishizaka J, Ikeda T, Takahashi MM (2002) Structure and size distribution of plankton communities down to the grater depths in the western North Pacific Ocean. Deep Sea Res II 49:5513–5530

Yokouchi K, Tsuda A, Kuwata A, Kawai H, Ichikawa T, Hirota Y, Adachi K, Asanuma I, Ishida H (2007) Simulated in situ measurements of primary production in Japanese waters. In: Kawahata H, Awaya Y (eds) Elsevier Oceanography Series 73, Global climate change and response of carbon cycle in the equatorial Pacific and Indian Oceans and adjacent landmasses, Elsevier science, Amsterdam, pp 65–88

Yoshikawa C, Abe H, Aita MN, Breider F, Kuzunuki K, Toyoda S, Ogawa NO, Suga H, Ohkouchi N, Danielache SO, Wakita M, Honda MC, Yoshida N (2016) Insights into the production processes of nitrous oxide in the western north Pacific by using a marine ecosystem isotopomer model. J Oceanogr 72:491–508. doi:10.1007/s10872-015-0308-2

Zeng J, Nojiri Y, Murphy PP, Wong CS, Fujinuma Y (2002) A comparison of ΔpCO2 distributions in the northern North Pacific using results from a commercial vessel in 1995–1999. Deep Sea Res II 49:5303–5315